Metal–Air Batteries with High Energy Density: Li–Air versus Zn–Air

Jang-Soo Lee, Sun Tai Kim, Ruiguo Cao, Nam-Soon Choi, Meilin Liu, Kyu Tae Lee, and Jaephil Cho**

In the past decade, there have been exciting developments in the field of lithium ion batteries as energy storage devices, resulting in the application of lithium ion batteries in areas ranging from small portable electric devices to large power systems such as hybrid electric vehicles. However, the maximum energy density of current lithium ion batteries having topatactic chemistry is not sufficient to meet the demands of new markets in such areas as electric vehicles. Therefore, new electrochemical systems with higher energy densities are being sought, and metal-air batteries with conversion chemistry are considered a promising candidate. More recently, promising electrochemical performance has driven much research interest in Li-air and Zn-air batteries. This review provides an overview of the fundamentals and recent progress in the area of Li-air and Zn-air batteries, with the aim of providing a better understanding of the new electrochemical systems.

1. Introduction

Fluctuation of oil prices and the effects of global warming have forced us to look for alternative energy storage and conversion systems, such as the smart grid. In addition, portable electronic equipment and devices have been developing at a rapid pace, and this progress demands ever-increasing energy and power density in power sources. Due to their energy density, which is higher than that of previous power sources such as Ni-MH batteries, lithium-ion batteries are being considered in the hope of being able to meet these demands. However, the maximum energy density of current lithium-ion batteries is limited owing to electrode materials having intercalation chemistry, and thus such batteries are not satisfactory for the practical application of electric vehicles. Therefore, metal-air batteries have attracted much attention as a possible alternative, because their energy density is extremely high compared to that of other rechargeable batteries, as shown in **Figure 1**.[1] A notable characteristic of metal-air batteries is their open cell structure, since these batteries use oxygen gas accessed from the air as their cathode material. The cell configuration of conventional rechargeable batteries is a closed system. There are several kinds of metal-air batteries based on different metal species; their reaction mechanisms are variable, resulting in requests for different types of cell components. Typically, metal-air batteries are divided into two types according to their electrolytes. One is a cell system using an aqueous electrolyte; such a system is not sensitive to moisture. The other is a water-sensitive system using an electrolyte with aprotic solvents. This system is degraded by moisture.

Among metal-air batteries, metals such as Ca, Al, Fe, Cd, and Zn are appropriate for the aqueous system. Zinc-air batteries in particular have powerful potential for use as alternative energy storage devices. Al can be more easily corroded than Zn in alkaline solution, although Al-air cells have a much greater energy density than zinc-air cells.[2] Also, Zn has various advantages such as low cost, abundance, low equilibrium potential, environmental benignity, a flat discharge voltage, and a long shelf-life.[3,4] The most important merit of alkaline zinc-air batteries, however, is that non-noble metal catalysts can be used for the oxygen reduction reaction. The theoretical specific energy density of Zn-air batteries is 1084 $Wh \cdot kg^{-1}$.

In 1996, Abraham et al. introduced a rechargeable Li-air battery; it was composed of a Li^+ conductive organic polymer electrolyte membrane, a Li metal anode, and a carbon composite electrode.[5] Li metal is explosively reactive with water, and thus a non-aqueous electrolyte is required. Oxygen is reduced on discharging to form Li_2O_2 or Li_2O. Then, the lithium oxides are electrochemically decomposed to Li and O_2 on charging. The specific energy density of Li-air batteries is 5200 $Wh \cdot kg^{-1}$ when the mass of oxygen is included. However, Li-air batteries did not attract wide attention when they were introduced, although they have much higher energy densities than those of conventional Li-ion battery systems (about 200–250 $Wh \cdot kg^{-1}$). In 2006, Li-air batteries were revisited by the Bruce group.[6] These researchers showed promising electrochemical performance for practical applications, and their work triggered new research into Li-air batteries.

To cover all metal-air batteries would be beyond the scope of this article. Zn-air and Li-air batteries have attracted the most

J.-S. Lee, S. T. Kim, Dr. R. Cao, Prof. N.-S. Choi, Prof. K. T. Lee, Prof. J. Cho
Interdisciplinary School of Green Energy
Ulsan National Institute of Science and Technology (UNIST)
Ulsan, 689–798, Korea
E-mail: ktlee@unist.ac.kr; jpcho@unist.ac.kr
M. Liu
School of Materials Science and Engineering
Georgia Institute of Technology
771 Ferst Drive, N.W. Atlanta, GA 30332–0245

DOI: 10.1002/aenm.201000010

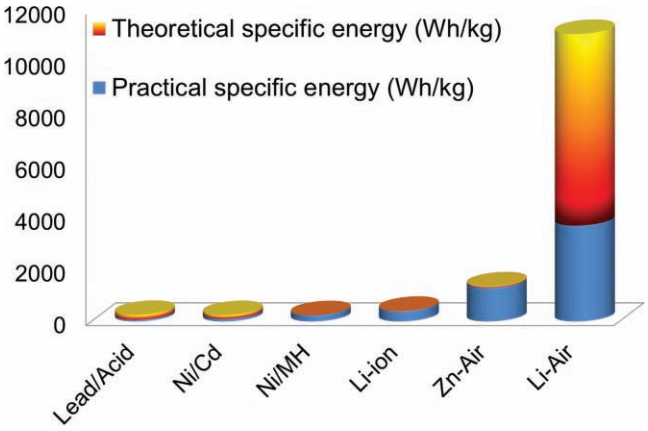

Figure 1. Theoretical and practical energy densities of various types of rechargeable battery.

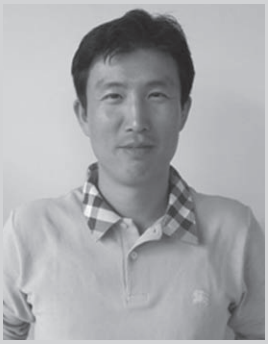

Jaephil Cho is a professor and a dean at the Interdisciplinary School of Green Energy at UNIST (Korea). He received his Ph.D. (1995) in Ceramic Engineering from Iowa State University (USA). He is a director of the Converging Research Center for Innovative Battery Technologies supported by the Ministry of Education, Science & Technology in Korea. His current research is focused mainly on nanomaterials for energy conversion and storage, nanoscale coatings, and safety enhancement of Li-ion batteries.

attention, therefore this review provides an overview of selected developments in the area of electrode and electrolyte materials for both Zn-air and Li-air batteries over the past decade, and particularly in the past few years. Also, this article focuses on major improvements in air cathodes, metal anodes, and electrolytes.

2. Li–Air Batteries

2.1. Configuration: Non-aqueous vs. Aqueous vs. Hybrid vs. All-Solid-State Electrolytes

There are four types of Li-air batteries, categorized according to the species of electrolyte: Li salts-dissolved in

i) nonaqueous (aprotic) solvents
ii) aqueous solvents
iii) hybrid (non-aqueous/aqueous) solvents, and
iv) all solid-state electrolyte.

All four systems use Li metal and oxygen gas as anode and cathode materials, respectively. However, their reaction mechanisms differ according to the electrolyte used. (**Figure 2**)

The configuration of the non-aqueous electrolyte system is similar to that of conventional Li-ion batteries. Conventional Li-ion batteries use carbon or alloy materials as anodes, Li metal oxides or phosphates as cathodes, and Li salt dissolved in aprotic solvents as electrolytes. Li-air batteries use oxygen gas as a cathode material and thus, porous carbon and catalyst composites must be added as the Li_2O_2 reservoir in the cathode. Also, Li metal must be used as the anode, because anodes play a role as the Li source in Li-air batteries. The critical difference between the two systems is that an open system is required to for Li-air batteries, because oxygen is obtained from the air. This open system requires additional components such as air-dehydration membranes.[7–9]

As mentioned above, the non-aqueous electrolyte system was first introduced by Abraham et al., and they suggested the following stepwise reaction mechanism.[5]

$$2Li + O_2 \rightarrow Li_2O_2 \qquad E^o = 3.10\ V\ vs.\ Li/Li^+$$

$$4Li + O_2 \rightarrow 2Li_2O \qquad E^o = 2.91\ V\ vs.\ Li/Li^+$$

Standard cell potentials, E^o, were calculated using the standard Gibbs free energy of formation. Then, the Bruce group demonstrated that Li_2O_2 is formed on charging and decomposes according to the reaction, $Li_2O_2 \rightarrow O_2 + 2Li^+ + 2e^-$, based on ex situ powder X-ray diffraction and in situ mass spectroscopy, as shown in **Figure 3**.[6] Recently, Lu et al. revised the theoretical reversible potentials of the above equations, as shown below. These values are derived from the published Gibbs free energies.[10]

$$2Li + O_2 \rightarrow Li_2O_2 \qquad E^o = 2.96\ V\ vs.\ Li/Li^+$$

$$4Li + O_2 \rightarrow 2Li_2O \qquad E^o = 2.91\ V\ vs.\ Li/Li^+$$

Recently, Laoire et al. carried out a fundamental study of the influence of solvents on the oxygen reduction reaction (ORR) to elucidate the reaction mechanism of the oxygen electrode.[11,12] Based on elelectrochemical analysis and XRD experiments, they suggested the following O_2 reduction processes.

$$Li^+ + e^- + O_2 \rightarrow LiO_2 \qquad E^o = 3.0\ V\ vs.\ Li/Li^+$$

$$2LiO_2 \rightarrow Li_2O + O_2 \quad \text{(chemical reaction)}$$

$$Li^+ + e^- + LiO_2 \rightarrow Li_2O_2 \qquad E^o = 2.96\ V\ vs.\ Li/Li^+$$

$$2Li^+ + e^- + Li_2O_2 \rightarrow 2Li_2O \qquad E^o = 2.91\ V\ vs.\ Li/Li^+$$

The oxygen reduction reaction proceeds in a stepwise fashion to form O_2^-, O_2^{2-}, and O^{2-} as products, and the first product of the reduction of oxygen is lithium superoxide, LiO_2, involving a one electron process. These reactions are kinetically irreversible or quasi-reversible electrochemical processes, resulting in high polarization for the oxygen evolution reaction. Also, Laoire et al. reported that solvents have significant influence on kinetics.

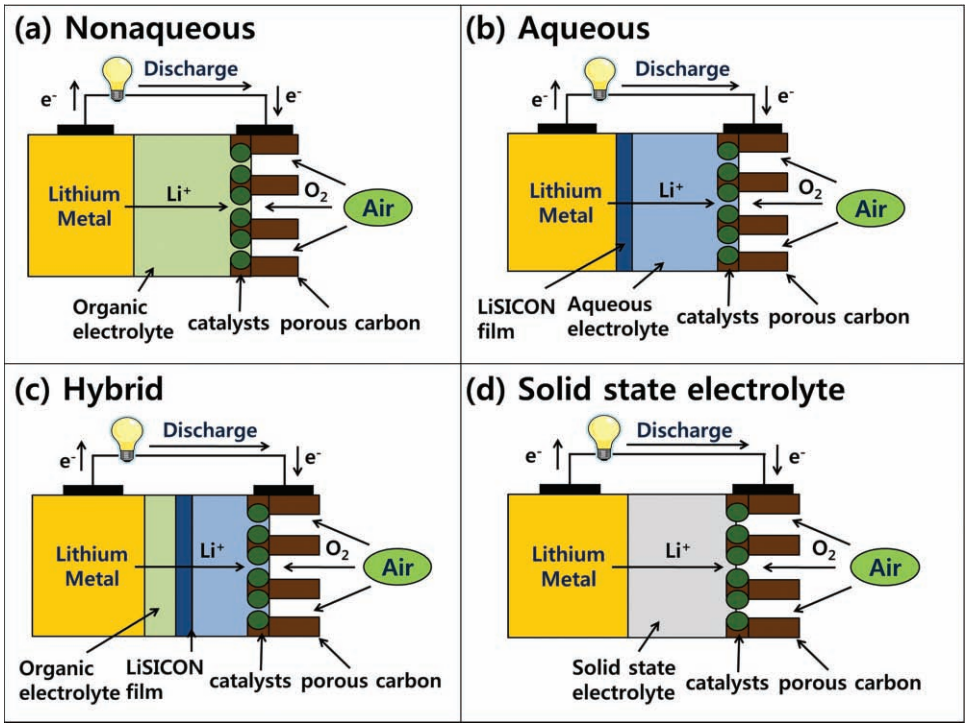

Figure 2. Schematic cell configurations for the four types of Li-air battery.

High donation number solvents provide increased stability for the complex $[Li^+(solvent)_n—O_2^-]$ due to the modulated Lewis acidity of the hard acid. This suggests that the O_2/O_2^- reversible couple may be seen in solvents with high donation numbers. In solvents with low donation numbers, O_2^- tends to decompose or to undergo fast electrochemical reduction to O_2^{2-}; this means that O_2 may be fully reduced to O^{2-}. A reaction mechanism similar to that of LiO_2 formation was also addressed based on density functional theory calculations by Hummelshoj et al.[13] Recently, Mizuno et al. and Lu et al. pointed out that the high reactivity of superoxide species induces the additional reaction mechanism.[14,15] The superoxide species can be reacted with aprotic solvents to form RO-(C = O)-OLi (R = alkyl group).[16,17] Mizuno et al. suggested that this reaction is reversible based on SAED (selected area electron diffraction), EDXS (energy dispersive x-ray spectroscopy), and EELS (electron energy loss spectroscopy) analysis on the discharge products, but the polarization of its decomposition is higher than that of Li_2O_2.[14] This implies that an additional catalyst is required for the oxygen reduction and evolution reactions, since previous catalysts were designed to be effective for the direct formation and decomposition of Li_2O_2.

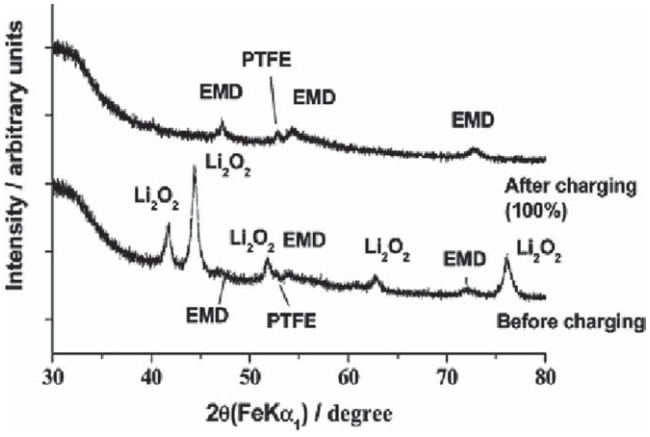

Figure 3. Powder X-ray diffraction data for a Li_2O_2/Super S/EMD/PTFE electrode before charging and after passage of sufficient charge to decompose all the Li_2O_2. Reprinted with permission.[6] Copyright 2006, American Chemical Society.

In 2004, Polyplus Co. introduced a protective glass-ceramic layer for Li metal (LiSICON, $LiM_2(PO_4)_3$); this layer enables Li metal to remain stable in water.[18] The layer is ionically conductive, and prevents vigorous reactions with water. Thus, Polyplus essentially developed Li-air batteries using an aqueous electrolyte.[19] The aqueous electrolyte system is composed of the protected Li metal anode, the aqueous electrolyte, and the air cathode. The reaction mechanisms for aqueous Li-air batteries are different from those for non-aqueous Li-air batteries.

$$4Li + O_2 + 2H_2O = 4LiOH \quad \text{(in a basic electrolyte)}$$

$$4Li + O_2 + 4H^+ = 4LiOH + 2H_2O + Li \quad \text{(in an acidic electrolyte)}$$

Polyplus also showed a hybrid version of an aqueous electrolyte, with Li anode//non-aqueous electrolyte/ionic conducting glass-ceramic membrane/aqueous electrolyte//air cathode. The hybrid electrolyte system was also introduced by the Zhou group.[20,21] They also used the hybrid electrolyte, 1 M $LiClO_4$ in

ethylene carbonate + dimethyl carbonate and 1 M KOH aqueous solution, separated by a LISICON ($Li_{1+x+y}Al_xTi_{2-x}Si_yP_{3-y}O_{12}$) film.

Various ionic conducting glass-ceramic protective double layers have been introduced to improve the charge -ransfer reaction of Li ions between Li metal and aqueous electrolytes.[22–25] The Imanishi group reported that $Li_{1+x+y}Al_xTi_{2-x}Si_yP_{3-y}O_{12}$ was stable in water, but is reactive with Li metal. However, a glass-ceramic $Li_{3-x}PO_{4-y}N_y$ (LiPON) and a lithium-conducting polymer electrolyte (PEO_{18}LiTFSI) inhibited the direct reaction of Li and LATP. Therefore, the Imanishi group used a double layer of LiPON//LATP or PEO_{18}LiTFSI//LATP for aqueous Li-air batteries.

Recently, a totally solid-state Li-air battery was demonstrated by Kumar et al.[26] The cell is composed of an Li metal anode, an Li-ion conductive solid electrolyte membrane laminate fabricated from glass-ceramic and polymer-ceramic materials, and a solid-state composite air cathode prepared from high-surface-area carbon and ionically conductive glass-ceramic powder. The sample exhibited good thermal stability and rechargeability in the range of 30–105 °C.

All of the above systems are considered to be promising, and much attention has been attracted by all species of Li-air batteries. However, many problems still need to be solved and practical issues need to be addressed. In light of this, this review will focus on Li-air batteries using a non-aqueous electrolyte, as the non-aqueous electrolyte system seems to be further advanced than the others.

2.2. Air Cathode

2.2.1. Electrode Architecture

The air cathode is composed of carbon, a catalyst, and a polymer binder. The electrode architecture affects the electrochemical performance, as it does in a hydrogen fuel cell, because the reaction mechanisms of Li-air batteries and that of fuel cells are similar. In the case of hydrogen fuel cells, H^+ protons move through the electrolytes to meet oxide ions at the catalyst to form water. In the case of Li-air batteries, Li^+ ions move through the electrolytes and meet oxide ions at the air cathode surface to form a Li_2O_2 precipitate. The differences between Li-air batteries and hydrogen fuel cells are: i) the reduction reaction of oxygen can happen without catalysts in Li-air batteries, but such non-catalyzed reactions are not possible for fuel cells; ii) the reduced product of oxygen in Li-air batteries is accumulated as a solid in the pores of the cathode electrode, but the reduced product of oxygen in the fuel cells is not accumulated because it forms water.

The pores of air cathodes in Li-air batteries become increasingly blocked by Li_2O_2 precipitates as the discharge proceeds. This finding is supported by impedance analysis, as the pore blocking causes an increase of cell resistance because oxygen gas diffusion is not facilitated.[27–29] The microstructure of carbon materials is thus a critical factor that affects the electrochemical performance of Li-air batteries.

Cheng et al. and Xiao et al. investigated various carbon materials with different surface areas to determine their effect on specific capacity.[30,31] The specific capacity is proportional to the surface area, because the surface area of the carbon dictates the number of the electrochemical active sites available to form lithium oxides. This means that carbon with a higher surface area is beneficial for obtaining higher specific capacity. However, higher surface area does not always mean better performance. The more important factor is pore size. When the pore size is too small, such as with micropores, the entrance of the pores is easily blocked, and the inner part of the pores cannot then be utilized for their electrochemical active sites, resulting in poor specific capacity. Yang et al. investigated various carbon materials with different pore sizes and surface areas to determine the effect of these factors on specific capacity.[32] A mesoporous mesocellular carbon foam delivered higher specific capacity due to its pore size (ca. 30 nm), which is larger than that of other carbon materials even though the foam has a smaller surface area. However, if the pore size is too large, the volumetric energy density of the air electrode decreases, as suggested by theoretical calculations.[33] Therefore, the pore size should be optimized to exhibit better performance; there is a trade-off between carbon surface area and pore size.

The thickness of the air electrodes plays another important role in electrochemical performance. Zhang et al. reported that thicker electrodes delivered lower specific capacity.[34] This performance is attributed to slow oxygen diffusion through electrodes immersed in electrolytes. Scanning electron microscopy (SEM) images of the surfaces of the air electrode of a fully discharged cell showed that the voids on the air side were almost fully filled by solid deposition; however, the voids on the separator side were still wide open. Beattie et al. found that a higher specific capacity is delivered as the loading amount of carbon is decreased.[35] The electrode delivered about 6000 $mAhg^{-1}$ when 1.9 mg of carbon was loaded on the circular nickel foam disk (7/16 in. diameter). The mass-transfer limiting of oxygen diffusion can also be explained by the mathematical diffusion-limited model.[36,37] This model predicts that the partial pressure of oxygen affects the electrochemical performance. Oxygen diffusion through the air electrode was considered to be facilitated by increasing oxygen pressure. Read et al, Yang et al. and Tran et al. showed that the specific capacity increased as the oxygen pressure increased.[38–40] This phenomenon indicates that practical application of Li-air batteries will not be easy. Most studies on Li-air batteries have been performed using pure oxygen gas, and, therefore, oxygen pressure is 1 atm. However, the oxygen partial pressure of air is about 0.2 atm, much lower than that of pure oxygen gas.[9]

The effect of the electrode composition on the specific capacity has also been addressed.[35] Different ratios of carbon, catalyst, and binder induce different porosities, wettablility of electrolytes, and electrical contact of active materials, resulting in variable electrochemical performance. In addition, the optimum conditions for electrode composition are dependent on the species of carbon, the catalyst, and the binder.

2.2.2. Catalyst

A few reports on catalysts for Li-air batteries have been published. The Bruce group have investigated the effect of various catalysts on electrochemical performance.[41] This group examined the use of Pt, $La_{0.8}Sr_{0.2}MnO_3$, Fe_2O_3, NiO, Fe_3O_4, Co_3O_4,

CuO, and $CoFe_2O_4$ bulk materials (1–5 μm) as catalysts. The oxygen reduction reaction (ORR) and oxygen evolution reaction (OER) can take place even in the absence of a catalyst, as reported. However, catalysts can facilitate both reactions, although it is clear that the discharge voltage is little affected by catalysts. For examples, the charge voltage, the discharge capacity, and the capacity retention are substantially dependent on the catalyst used. The OER occurs at around 4.8 V *vs.* Li/Li^+ without a catalyst, which is lower than the redox potential of electrolyte decomposition (5.1 V). When Co_3O_4 was used as a catalyst, the redox potential of OER was shifted to a significantly lower voltage, ca. 4.0 V. The Fe_2O_3 catalyst delivered the highest capacity, and the Fe_3O_4, Co_3O_4, CuO, and $CoFe_2O_4$ catalysts exhibited more stable cycle performances.

This group also investigated various nanostructured manganese oxide catalysts, such as α-MnO_2, β-MnO_2, λ-MnO_2, electrolytic manganese oxide (EMD), Mn_2O_3 and Mn_3O_4.[42] Among them, α-MnO_2 nanowires showed the best electrochemical performance, delivering about 3000 $mAhg^{-1}$ at a current density of 75 mAg^{-1}, and showing a stable cycle performance for 10 cycles (**Figure 4**). This group suggested that the improvement is due to the crystal structure having 2 × 2 tunnels formed by edge- and corner-sharing MnO_6 octahedra. Li_2O can be incorporated within the tunnels, with O^{2-} ions located at the tunnel centers and the Li^+ ions coordinated between these central O^{2-} ions and those forming the walls of the tunnels. The ability to accommodate both Li^+ and O^{2-} within the tunnels suggests the possibility of incorporating Li^+ and O^{2-}. Such incorporation is not possible in other manganese oxide materials. The redox potentials of ORR and OER were 2.75 and 4.0 V vs. Li/Li^+, respectively, when α-MnO_2 nanowires were used. The polarization of oxygen evolution reaction (OER) was much higher than that of ORR, as the equilibrium redox potential is 2.9 V. This indicates that manganese oxide catalysts are effective for ORR, but are less effective for OER.

Recently, the Shao-Horn group reported that ORR and OER require different catalysts due to their different catalytic mechanisms.[10] For example, Pt was more effective for OER and Au was more effective for ORR. The redox potential of OER was 3.8 V vs. Li/Li^+ when Pt was used. The redox potential of ORR was 2.7 V vs. Li/Li^+ when Au was used. The current density was 250 mAg^{-1}. The polarization of ORR and OER was substantially decreased by Au and Pt catalysts, respectively. However, Pt and Au were not effective at decreasing the polarization of ORR and OER, respectively. This result is contrary to the case for the hydrogen ORR. It is known that Pt is more effective for H-ORR than Au. Pt is known to be a good catalyst for the complete reduction of O_2 to water, whereas Au has high selectivity for H_2O_2 due to its poor ability to break O–O bonds. Based on theoretical calculations, Xu et al. explained why the intrinsic catalytic reactivity of Pt (111) renders it less effective for Li-ORR than Au(111).[43] Periodic density functional theory (DFT) calculations were performed in a generalized gradient approximation using the Vienna ab initio simulation package. These researchers suggested that Pt (111) is expected to have a lower reversible potential than Au (111) because Pt stabilizes O more than it stabilizes lithium oxide species when compared to Au.

The Shao-Horn group further developed a catalyst for OER and ORR in Li-air batteries, based on their previous studies.[44] They introduced a bifunctional electrocatalyst, $Pt_{0.5}Au_{0.5}$ (PtAu)

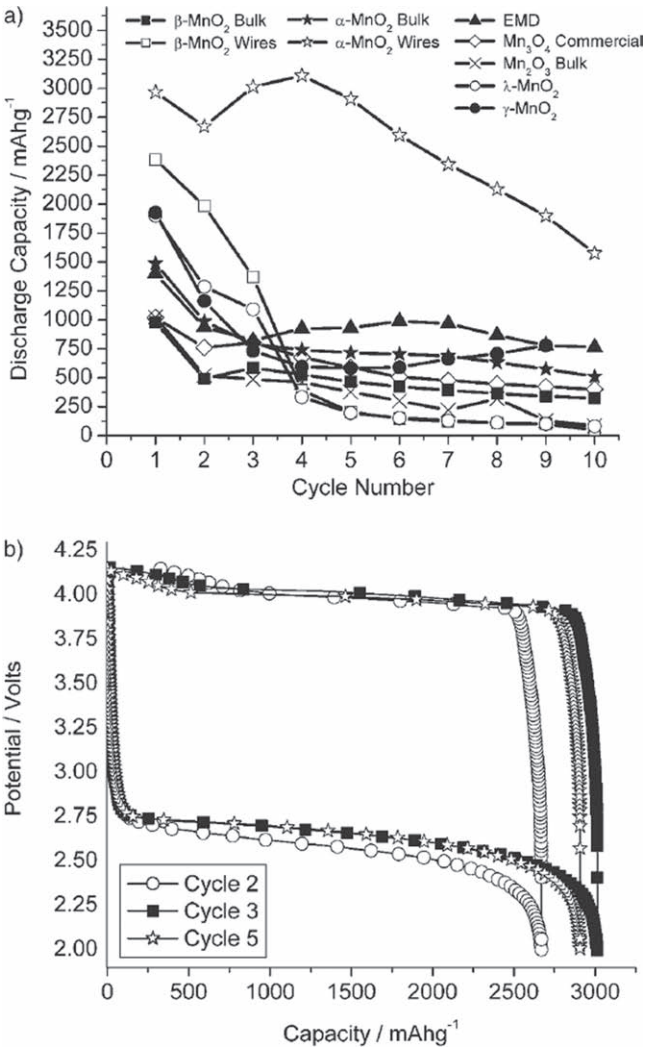

Figure 4. a) Variation of discharge capacity with cycle number for several porous electrodes containing manganese oxides as catalysts. b) Variation of potential with state of charge for a porous electrode containing α-MnO_2 nanowires. Reprinted with permission.[41] Copyright 2007, Elsevier.

nanoparticles (**Figure 5**). PtAu nanoparticles (6–7 nm diameter) were synthesized by reducing $HAuCl_4$ and H_2PtCl_6 in oleylamine and then loaded onto Vulcan carbon to yield 40 wt% PtAu/C. Interestingly, the PtAu catalyst exhibited ORR (ca. 2.7 V) and OER (ca. 3.6 V) voltages comparable to those of Au (ca. 2.7 V) and Pt (ca. 3.6 V) catalysts, respectively, when the current density was 100 mAg^{-1}. This indicates that surface Pt and Au atoms on PtAu/C are responsible for ORR and OER kinetics, respectively. Also, it is notable that the PtAu catalyst exhibited lower OER voltages than metal oxide catalysts such as α-MnO_2 and Co_3O_4. The lowest OER potential we know of is 3.6 V for pyrolyzed cobalt phthalocyanine supported on carbon.

2.3. Electrolyte

Read reported the influence of various electrolytes on electrochemical performance in 2002.[45] He investigated $LiPF_6$

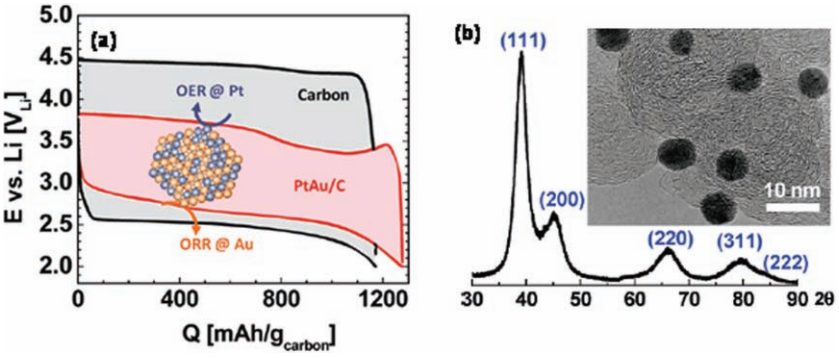

Figure 5. a) Li-O_2 cell discharge/charge profiles of carbon (black, 85 mA/g_{carbon}) and PtAu/C (red, 100 mA/g_{carbon}) in the third cycle at 0.04 mA/cm^2 electrode. b) Representative TEM image (top right) and XRD data of PtAu/C. Reprinted with permission.[44] Copyright 2010, American Chemical Society.

salt dissolved in various solvents such as PC, λ-BL, EC, DEC, DMC, DME, THF, THP, and their combinations. PC, λ-BL, EC, DEC, DMC, DME, THF, and THP denote propylene carbonate, λ-butyrolactone, ethylene carbonate, diethyl carbonate, dimethyl carbonate, 1,2-dimethoxyethane, tetrahydrofuran, and tetrahydropyran, respectively. He suggested that oxygen solubility in the electrolyte was correlated to the discharge capacity. Electrolytes with high oxygen solubility result in high discharge capacity. The PC:DEC (1:1) solvent exhibited the highest discharge capacity, 2120 $mAhg^{-1}$. Read et al. considered not only oxygen solubility but also electrolyte viscosity.[38] The discharge capacity was increased by decreasing electrolyte viscosity. This indicates that lower viscosity facilitates oxygen transport in the electrolyte, resulting in improving ORR kinetics.

Recently, Xu et al. suggested that electrolyte polarity is a more important factor in affecting the electrochemical performance than the oxygen solubility in the electrolyte.[44,46] Also, they addressed the fact that the effect of electrolyte viscosity and conductivity on the performance is limited. The oxygen diffusion rate through the open channels is several orders of magnitude higher than that through the liquid electrolyte. The open channels are strongly dependent on the polarity of the electrolytes. The air electrodes are composed of carbon materials, which have low polarity and hydrophobic properties. Thus, an electrolyte based on ethers and glymes can easily wet the carbon surface of the air electrode, because these electrolytes have low polarity as well. The air electrode is highly porous, and the pores are infiltrated by electrolytes. In other words, the electrolyte may easily flood all the pores inside the air electrode when the electrolyte has good wetting properties for the carbon surface. This result is deduced from the triphase model for oxygen reduction. The triphase model shows that oxygen reduction in the air electrode occurs in the triphase regions where the gas (oxygen), liquid (electrolyte), and solid (carbon and catalyst) exist.

However, Zhang et al. also suggested that the oxygen reduction reaction occurs in two phase regions where liquid (electrolyte) and solid (catalyst/carbon) are present.[47] According to this model, they insisted that the air electrode should be completely wetted with the liquid electrolyte to supply the maximum reaction area for a high specific capacity. Meanwhile, they also suggested that the air electrode should not be flooded by the liquid electrolyte so that the air electrode has enough pores for the fast oxygen gas diffusion to obtain good rate capability. Therefore, the status of electrolyte-filling plays an important role in the specific capacity and rate capability, because the empty pores have a trade-off between the electrochemical active sites and oxygen diffusion channels. In this regard, a hybrid air electrode is considered to form air-flow channel by Xiao et al. The hybrid electrode is composed of a conventional air electrode and extremely hydrophobic CF_x, which facilitates the formation of air-flow channels in the carbon matrix. It alleviates the pore blocking problem caused by lithium oxide deposits.[48]

Hydrophobic ionic liquid electrolytes have been considered promising for Li-air batteries. Certain ionic liquids such as 1-ethyl-3methylimidazolium bis(trifluoromethylsulfonyl)amide (EMITFSI) are almost immiscible in water.[49] This immiscibility is beneficial for electrolytes of Li-air batteries. Moisture in the air can diffuse to the Li metal anode through the conventional electrolyte, resulting in chemical oxidation of Li metal on the anode surface. That is why the hydrophobic membranes are added to cover the air cathode, to inhibit water invasion in the electrolyte. Also, ionic liquids do not evaporate at room temperature due to low vapor pressure. This property is also an appropriate electrolyte for Li-air batteries. As Li-air batteries are an open system, the carbonate solvents of conventional electrolytes can be evaporated, resulting in a change in the concentration of the electrolytes. Kuboki et al. investigated ionic liquid electrolytes consisting of 1-alkyl-3-methyl imidazolium cation and perfluoroalkylsulfonyl imide anion.[50] The resulting battery delivered 5360 $mAhg^{-1}$, and worked for 56 days in air. Also, Zhang et al. examined the ionic liquid-silica-Poly(vinylidene fluoride-*co*-hexafluoropropylene) (PVdF-HFP) polymer composite electrolyte as a waterproof electrolyte. The ionic liquid was 1,2-dimethyl-3-propylimidazolium bis(trifluoromethanesulfonyl) imide (PMMITFSI).[51]

2.4. Li Metal Anode

2.4.1. Degradation

A lithium electrode is expected to achieve a high energy density due to its having the most electropositivity (−3.04 V vs. standard hydrogen electrode) and the lightest metal (equivalent weight = 6.94 $gmol^{-1}$, specific gravity = 0.53 gcm^{-3}); it also has a high specific capacity (3860 $Ahkg^{-1}$).[52] However, the combination of lithium metal and a liquid electrolyte solution is very problematic for rechargeable batteries because of the high reactivity of the active lithium metal with any relevant polar aprotic solvent and/or salt anion in electrolyte solutions. Peled et al. suggested that the surface reaction of lithium metal with electrolyte components results in the formation of a mosaic structure of insoluble surface species and thus the solid electrolyte interphase

(SEI) layer formed on lithium has a multilayer structure.[53,54] The morphology for lithium deposition is dendritic and very porous, and the dendritic lithium can be cut and isolated from the anode substrate during the discharge. This isolated lithium causes a loss of anode materials and leads to a shorter cycle life. Therefore, dendritic lithium formation and the electrochemical instability of a lithium metal electrode still remain significant challenges that must be overcome to allow the operation of Li-air batteries. It should be noted that the surface of the metallic lithium electrode is covered with a 'native layer' consisting of various lithium compounds such as LiOH, Li_2O, Li_3N, or Li_2CO_3. These compounds are produced by the reaction of metallic lithium with O_2, H_2O, CO_2, or N_2; the compounds can be detected by X-ray photoelectron spectroscopy (XPS).[55,56] It is known that the inner and outer layer of a native layer mainly consist of Li_2O and $LiOH/Li_2CO_3$, respectively. In contact with electrolytes, an SEI layer is spontaneously formed by the reductive decomposition reactions of organic solvents, salt, and impurities with a lithium electrode; these reactions protect the lithium metal from further degradation.[57] During the lithium stripping process, the lithium ion transfers from the SEI layer to the electrolyte solution by passing through the SEI. The kinetic energy needed to complete this process will be quite different depending on the composition of the SEI. In other words, if the ionic resistance of the SEI is high, high activation energy is required for a lithium ion to pass through it. It is generally accepted that the SEI consists of two layers: i) an inorganic phase based on lithium compounds such as LiF, Li_2CO_3, etc., and ii) an organic phase composed of lithium compounds with various hydrocarbon moieties from organic solvents in the electrolyte.[58–61] The structure of the SEI layer, which acts as an interphase between the lithium electrode and the electrolyte, changes to a more complex morphology with the repeated cycling. The electrochemically stable SEI layer on the lithium electrode surface can diminish unexpected electrochemical behaviors such as low cycling efficiency, gradual capacity loss, and poor cycleability.[62,63]

The SEI layer on the lithium electrode cannot properly accommodate the dramatic morphological changes of the lithium metal upon lithium deposition and dissolution due to the non-uniformity of these processes under high current density (**Figure 6**).[64] The SEI layer can be easily cracked and broken during lithium deposition and dissolution. This behavior results in a considerable loss of active lithium metal and solution components due to the complex surface reactions and eventually leads to degradation of the lithium electrode. Moreover, the non-uniform current distribution of the lithium electrode, which is closely linked to the heterogeneous composition of the native layer, leads to dendritic lithium formation, provoking an internal short circuit in Li-air batteries.[65,66] Furthermore, it is known that nonuniform current density distribution can cause a sharp increase in local current density at the edge of a lithium anode. This produces an unusual exothermic condition, and runs the risk of explosions under any conditions of abuse. Therefore, it is extremely important to control the lithium electrode-electrolyte interface to successfully attain Li-air batteries with high energy density, good cycling efficiency, and superior safety. The rate-determining step for the charge-transfer reaction is associated with the ionic transport properties through the SEI layer. Whatever the nature and morphology of SEI layers, their presence modulates the electrochemical performances of lithium electrodes.[67] Actually, when pressure is applied to lithium electrodes in solutions (e.g., by packing Li batteries with external physical pressure, so that the separator between the lithium anode and the cathode pressurizes the lithium surface), phenomena such as dendritic lithium deposition can be drastically excluded.[68–70]

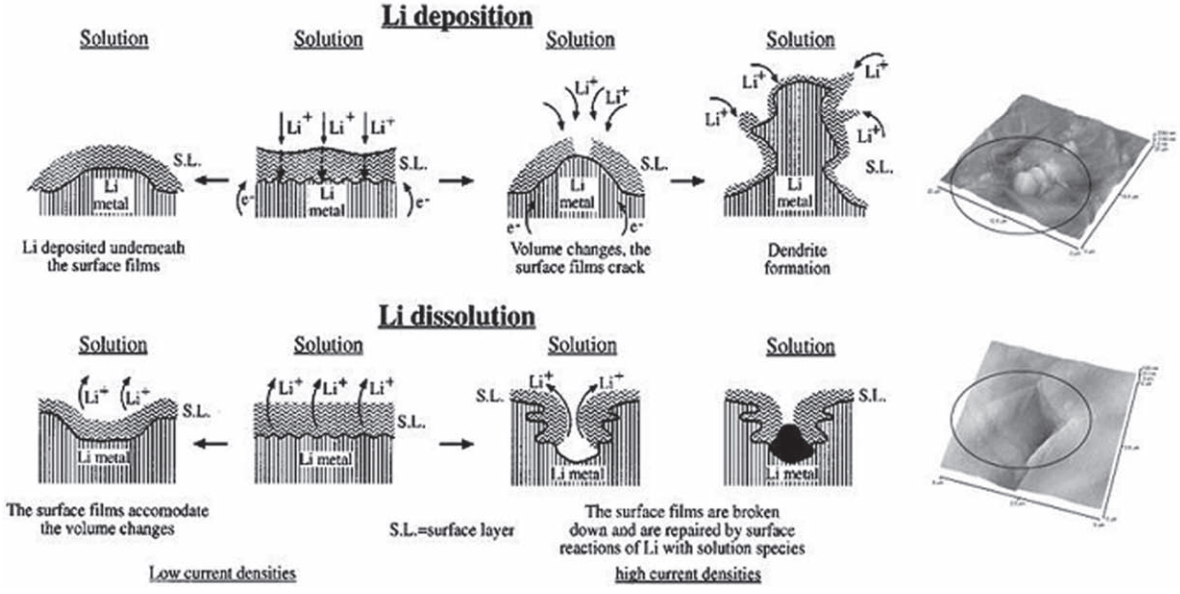

Figure 6. A description of the morphology and failure mechanisms of lithium electrodes during Li deposition and dissolution, and relevant AFM images (Li electrodes in an EC-DMC/$LiPF_6$ solution). Reprinted with permission.[64] Copyright 2000, American Chemical Society.

2.4.2. Surface Modification

Here we discuss intriguing work on the improvement of the interfacial properties of lithium metal electrodes. It has been reported that the modification of the lithium electrode surface affects lithium dendrite formation and electrochemical performance, including lithium cycling efficiency and cycleability. Much effort has been exerted to improve the surface uniformity of SEI layers and to form electrochemically stable SEI layers. Several approaches have been pursued to improve the rechargeability and reliability of the metallic lithium electrode: i) the use of liquid or polymer electrolytes that are less reactive toward lithium electrodes;[71–77] ii) the protection of lithium electrodes by adding surface active agents such as hydrocarbons and quarternary ammonium salts;[78,79] iii) the formation of Li_2CO_3, LiF, LiOH, or polysulfide by using CO_2,[74,80–86] HF,[87–90] water trace,[74,81,91] and S_x^{2-};[80,92] iv) the formation of a stable metal alloy (LiI) by incorporating SnI_2 or AlI_3;[93] v) the use of surfactants such as non-ionic polyether compounds;[94] vi) uniform lithium deposition by means of pressure and temperature;[70,95,96] vii) the removal of impurities from the interface of lithium metal and electrolyte with an inorganic filler such as silica, alumina, zeolite, or titanate,[97–102] viii) the suppression of lithium dendrites by the formation of an ultra-thin polymer electrolyte layer based on plasma polymerization or UV irradiation polymerization.[103–107]

The formation of a stable SEI layer on the lithium metal surface can be promoted by adding agents such as CO_2, HF, or S_x^{2-}, and, thus, the dendritic lithium formation can be greatly suppressed. In the presence of CO_2 in electrolytes, the inner layer of the SEI contains Li_2CO_3 and produces a smoother surface film on the lithium electrode.[108] Takehara et al. reported that the lithium deposited on a nickel substrate in HF-containing electrolytes had a hemispherical form and dendritic lithium was not observed.[55] This indicates that the addition of a small amount of HF to the electrolyte alters the composition of the SEI layer. They found that HF addition causes a smoothing of the Li metal surface, as a result of coverage mainly with LiF.[87,89,90,109,110] It should be noted that the surface of as-received lithium foils is essentially composed of LiF by acid-base reactions of HF with various basic lithium compounds (Li_2CO_3, LiOH, Li_2O) in a native layer.[110,111] It is believed that a dense and rigid LiF-based SEI layer leads to the reduction of reactivity of lithium electrodes toward electrolytes and inhibition of dendritic lithium formation.

SnI_2 and AlI_3 were also proposed as promising additives for improving lithium rechargeability.[93] Both Sn and Al are known to form lithium alloys. It is postulated that the thin layers of the lithium alloys at the lithium electrode surface cause an improvement of Coulombic efficiency during lithium deposition and dissolution. Also, when a polyether surfactant such as poly(ethylene glycol)dimethyl ether (PEGDME) was used as an additive, significant suppression of the inactivation of the deposited lithium was reported.[94] It was reported that the adsorption and desorption process of the surfactants accompanying lithium deposition-dissolution makes the current density more uniform on the lithium surface.

The crucial effect of physical factors such as temperature and pressure on the improvement of lithium cycling performance was investigated.[70,96] The suppression of dendritic lithium growth by using mechanical pressure was achieved. This is because lithium was deposited densely and uniformly on the lithium electrode surface under pressure and the isolation of deposited lithium from the electrode during the lithium stripping process was effectively reduced. In addition, low-temperature conditions could improve the cycling efficiency of lithium on the nickel substrate.

The addition of inorganic fillers such as SiO_2 or Al_2O_3 could enhance the interfacial stability of lithium electrodes due to their ability to trap liquid impurities.[97–102] Another approach for the build-up of a desirable SEI layer has been to form an ultra-thin plasma polymer layer on the lithium anode surface.[103] The surface of the lithium electrodes was covered with an ultra-thin and uniform solid polymer electrolyte layer that was prepared via plasma polymerization of 1,1-difluoroethene. Covering the lithium electrode surface with a solid polymer electrolyte can be one of the most effective ways to inhibit the dendritic growth of lithium and stabilize the lithium-electrolyte interface. In this regard, the use of a polymer electrolyte is expected to be both less reactive than the use of a liquid electrolyte and to accommodate interfacial volume change upon repeated charge and discharge processes. The low surface energy of the deposited plasma polymers contributed to a suppression of the growth of dendrites.

The effect of the protective layer on the cycleability as well as on the morphology and the composition of the SEI layers was investigated.[103–107] The formation of a semi-interpenetrating network (IPN) structure protective layer on lithium metal electrodes was attempted to make the lithium deposition morphology less dendritic. The UV-curable formulation consists of a curable monomer (1,6-hexanediol diacrylate), polymer solution (Kynar 2801 dissolved in purified tetrahydrofuran), liquid electrolyte (150 wt% EC/PC/1M $LiClO_4$ based on curable monomer), and photoinitiator (methyl benzoylformate, 2 wt% based on curable monomer) undergoing a fast cleavage upon photolysis to generate free radicals. A curable mixed solution was directly coated on the lithium metal surface and after drying it was irradiated with UV light for 2 min.[106] Then, a protective layer based on semi-IPN structure was formed on the lithium electrode surface.

3. Zn-air Batteries

Zinc-air cells are composed of three parts; zinc metal as an anode, an air electrode as the cathode, which is divided into a gas diffusion layer and a catalytic active layer, and a separator, as shown in **Figure 7**. Because the solubility of oxygen is very low at atmospheric pressure, it is necessary to use oxygen in the gas phase, not liquid.[112,113] Oxygen from the atmosphere diffuses into the porous carbon electrode by difference in pressure of oxygen between the outside and inside of the cell, and then the catalyst facilitates the reduction of oxygen to hydroxyl ions in the alkaline electrolyte with electrons generated from the oxidation of zinc metal as the anode reaction. This is why we call this process a three-phase reaction: catalyst (solid), electrolyte (liquid), and oxygen (gas). Note in Figure 7 the red circle where this three phase reaction occurs. This structure favors the gain of oxygen in zinc-air batteries. Generated hydroxyl ions migrate from the air cathode to the zinc anode to

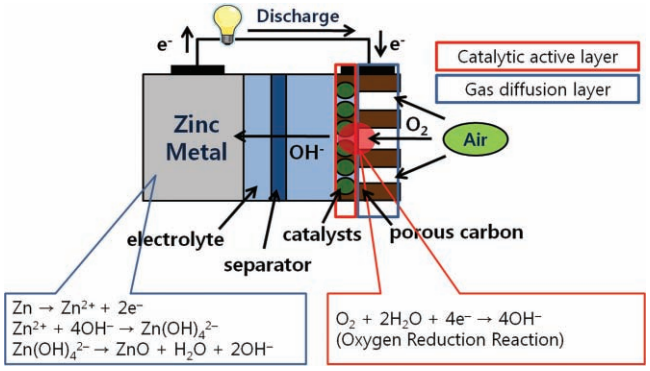

Figure 7. Working principle and each electrode reaction of zinc-air battery. Note the red circle where three phase reaction (oxygen (gas), catalysts (solid) and electrolyte (liquid)) occur in air cathode.

complete the cell reaction; this overall procedure during discharge can be described as the following electrochemical reactions of anode and cathode in alkaline solution, respectively.

Anode: $Zn \rightarrow Zn^{2+} + 2e^-$

$Zn^{2+} + 4OH^- \rightarrow Zn(OH)_4^{2-}$

($E^o = -1.25$ V *vs.* NHE)

$Zn(OH)_4^{2-} \rightarrow ZnO + H_2O + 2OH^-$

$Zn + 2H_2O \rightarrow Zn(OH)_2 + H_2 \uparrow$ [114]

(also possible)

Cathode: $O_2 + 2H_2O + 4e^- \rightarrow 4OH^-$

($E^o = 0.4$ V *vs.* NHE)

Overall reaction: $2Zn + O_2 \rightarrow 2ZnO$ ($E^o = +1.65$ V)

From the above chemical equation, with the exception of HER (which will be discussed later), the equilibrium potential of the zinc-air cell should be 1.65 V, where $E_{eq} = E^0$ (cathode) – E^0 (anode). However, the practical working voltage of the zinc-air cell is less than 1.65 V due to the internal loss of the cell due to activation, and ohmic and concentration loss.[2] In this review, we will not discuss these kinds of electrochemical losses in detail. However, it may be helpful to understand the electrochemical behavior of zinc-air batteries through a schematic polarization curve of each anode and cathode reaction.

Figure 8 is a schematic potential (v)-current (i) curve to efficiently understand the major origin of potential loss in zinc-air cells using oxygen. Note that the overpotential at the zinc anode is relatively smaller than that at the air electrode; also, the cathodic current occurs at the cathode, the air electrode. Conversely the anodic current occurs at the anode, the zinc electrode, in the discharge (red line). Of course, each current direction is reversed upon charging (blue line). From the polarization curve, it is possible to see that a large overpotential (the green line in Figure 8) is needed to generate hydroxyl ions by oxygen reduction reaction (ORR). This is why the working voltage of the actual zinc-air cell (E_1, Figure 8, red line) is much smaller than 1.65 V, the open-circuit potential (OCV) (E_{eq}, black line). Considering the reverse reaction (the oxygen evolution reaction) (OER), a larger potential is needed for charging (Figure 8, blue line). From the brief discussion above, it can be seen that using the ORR has both positive and negative effects on zinc-air cells. The positive point enables this cell to have large energy density because of the lack of oxygen active material in the cell. We have already discussed this point. The negative point, conversely, forces the zinc-air cell to have significant potential loss, which eventually causes a decrease in the power density of the cell. This is why many studies have focused on how to minimize the large overpotential in the cathode reaction by developing new catalysts and modifying air electrode structures. Of course, when it comes to a primary zinc-air cell, it is not necessary to consider any problem in the zinc anode because the utilized zinc metal can be replaced with fresh metal via mechanical charging. However, for the purpose of developing an electrically rechargeable zinc-air battery, it is also important to study how to improve the electrochemical behavior of the zinc anode. Setting aside these two major drawbacks in zinc-air cells, other problems could still be obstacles in developing a secondary zinc-air battery. In this review, we will deal with selected efforts to overcome possible problems in zinc-air cells and also discuss how to approach the development of a secondary zinc-air battery.

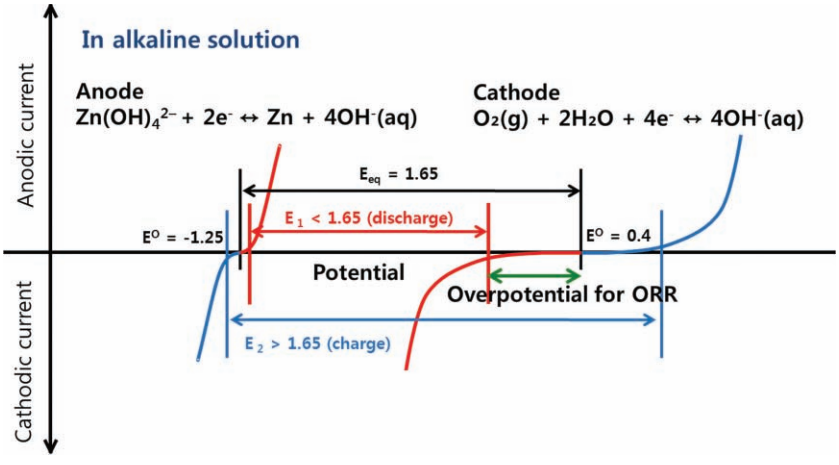

Figure 8. Schematic polarization curves of zinc-air cell. The equilibrium potential of the zinc-air cell (black line) is 1.65 V, but the practical voltage (red line) in discharge is lower than 1.65 V due to the sluggish ORR. A large potential is needed to charge zinc-air battery, higher than the equilibrium potential (blue line).

3.1. Anode: Zinc Electrode

Zinc-air batteries use pure zinc metal as an anode active material; oxidation of the zinc occurs during discharge. This is why most studies have focused on improving the air electrode, not the zinc anode. Although the zinc corrosion rate is slower than that

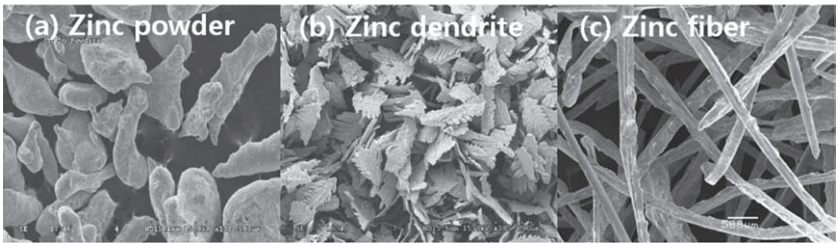

Figure 9. Various morphology of zinc metal. a) zinc powder, b) zinc dendrite and c) zinc fiber. Reprinted with permission.[118,119] Copyright 2002,2006, Elsevier.

of aluminum in an alkaline solution, this corrosion process generates hydrogen gas (hydrogen evolution reaction (HER)), according to $Zn + 2H_2O \rightarrow Zn(OH)_2 + H_2\uparrow$. Therefore, it is more reasonable to consider the electrochemical behavior of zinc metal in the alkaline electrolyte, not just the zinc metal in the gas phase. Because this HER is not supposed to occur during discharge, methods to retard the hydrogen evolution reaction have been regarded as the most important research area: it is hoped that it will be possible to consume zinc metal completely during discharge, which will eventually increase the capacity of the zinc-air battery.

As mentioned above, because zinc metal participates in the anode reaction during discharge, the most practical method of improving the performance of the zinc anode is to increase the surface area of the zinc particles so that the zinc can react with the alkaline electrolyte more efficiently. Accordingly, zinc particles with large surface area, such as Zn/MnO_2 and Zn/NiOOH[3] are the best choices, and morphology control of zinc metal, such as flakes[115] and ribbons[116] in alkaline zinc-MnO_2 cells and dendrites[117,118] and fibers[119] in zinc-air cells (see **Figure 9**)) have been reported. Although it is not precisely an example of a zinc-air cell, Minakshi et al. also showed that in the alkaline electrolyte LiOH, a porous anode electrode composed of zinc powder improves the rate capability and has a higher capacity in alkaline Zn-MnO_2 cells than that of a zinc planar electrode.[120] Recently, a study of porous electrodes with various shaped zinc particles, not just planar zinc electrodes, has also received attention.[121]

Generally, when preparing a zinc anode with powder, mercury has been added to the zinc anode to give better electrical conductivity between the zinc particles and the current collectors. However, removing the mercury in the zinc anode, necessary due to environmental problems, has negative effects on discharge performance, and results in leakage problems associated with hydrogen gas and shock resistance.[115] These problems can be alleviated fairly well by introducing gelling agents such as crosslinked carboxymethyl cellulose (CMC), starch graft copolymers, cross linked polyacrylic acid polymer[122] or organic binders.[123] Muller et al used cellulose as a gelling agent to optimize and stabilize the porosity of the zinc electrode,[124] and Othman et al. introduced hydroponics gels such as agar to increase the capability of storing electrolyte.[125]

When a porous zinc anode reacts with an alkaline electrolyte, the corrosion effect of the zinc metal can be another criterion for stabilizing a zinc anode with large surface area. Hydrogen evolution on the surface of the zinc anode deteriorates the utilization efficiency of the zinc, resulting both in increased internal pressure in the cell and water electrolysis. These side reactions eventually decrease the cycle life of a zinc-air battery.[126] Two methods to overcome hydrogen evolution have been studied in zinc-air batteries. One is to alloy the zinc with other metals (Hg, Pb, and Cd) with high hydrogen evolution overvoltage.[127,128] However, these toxic heavy metals cause another environmental problem. As an alternative, Lee et al. reported that alloying zinc metal with nickel and indium with different weight percentages is effective in shifting to more negative potentials for hydrogen evolution.[128] Zhang et al. suggested that introducing metallic bismuth to a pasted zinc electrode improved the discharge performance because of the formation of an electronic conductive material.[129]

Another method of suppressing hydrogen evolution is to coat the zinc metal with other materials; Cho et al. suggested that the zinc surface coated with Li_2O-$2B_2O_3$ (lithium boron oxide, LBO) could increase discharge capacity and decrease hydrogen evolution. It is believed that the coating layer prevents the zinc surface from facing the alkaline electrolyte directly, which enables the zinc to avoid side reactions in the cell.[130] Zhu et al. reported that neodymium conversion films have also been applied to coat pristine zinc metal depending on the ultrasonic impregnation method. Their work demonstrated a positive effect on increasing corrosion resistance, in turn stablizing the cycle behavior of the zinc electrode.[131] The other method is to put additives into the electrolytes to stabilize the zinc anode. Ein-Eli et al. introduced polyethylene glycol (PEG) and phosphate ester acid form (GAFAC RA600) as an organic corrosion inhibiter. Their results showed that PEG had better inhibiting properties than GAFAC RA600.[132] Using anions of organic acids,[126] and phosphoric acid, tartaric acid, succinic acid, and citric acid [133] exhibited positive effects on suppressing gas evolution and dendrite formation to some extent.

Making an electrically rechargeable zinc-air battery is still challenging. However, it still seems a worthwhile task to develop a secondary cell for practical use in the market if we consider the many advantages of a hypothetical zinc-air battery. Although a proper bifunctional catalyst is required to charge a zinc-air battery with lower electrical potential, it is also critical to make reversible zinc anode. It is well known that zinc metal undergoes shape changes such as the formation of dendrites in the charge-discharge cycling process.[3] Let us revisit anode reaction in discharge. Once a zinc-air battery starts to discharge, the following anode reactions occur in the alkaline solution:

$$Zn \rightarrow Zn^{2+} + 2e^-$$

$$Zn^{2+} + 4OH^- \rightarrow Zn(OH)_4^{2-}$$

$$(E^o = -1(25\ V\ vs.\ NHE)$$

$$Zn(OH)_4^{2-} \rightarrow ZnO + H_2O + 2OH^-$$

Zinc metal is oxidized to release electrons and forms the zinc(II) ion. Reaction (1) proceeds until the solubility of the zincate ion, $Zn(OH)_4^{2-}(aq)$, reaches a saturation point in

the hydroxide electrolyte. After exceeding this point, zincate ions are decomposed to ZnO, a white solid powder that acts as an insulater. Because supersaturation of the zincate ion in alkaline solution is time-dependent, it is very difficult to make a rechargeable zinc-air battery.[134] Therefore, understanding the chemistry of the zincate ion, $Zn(OH)_4^{2-}$(aq) in alkaline solution is necessary in order to develop a secondary zinc electrode. There have been several fundamental efforts to understand the behavior of the zincate ion in an alkaline electrolyte[3,135–138] and also to understand the electrodeposition of the zincate ion.[139–147] Dirkse suggested that $Zn(OH)_4^{2-}$, $Zn(OH)_3(H_2O)^-$, $Zn(OH)_2(H_2O)_2$ or polynuclear species may exist in supersaturated zincate solutions and that the existence of these species depends on the availability of OH^- and free H_2O molecules in the electrolyte.[137] Peng studied the mechanism of zinc electroplating and suggested that $Zn(OH)_2$ became $Zn(OH)_{ad}$ by gaining one electron and then $Zn(OH)_{ad}$ was reduced to Zn by gaining a second electron.[141] Einerhand et al. used a rotating ring disk electrode (RRDE) to determine the amount of hydrogen produced from the electrodeposition of zinc in alkaline solution and showed that hydrogen evolution increased with decreasing concentration of KOH and zincate.[144]

3.2. Separator and Electrolyte

3.2.1. Separator

The function of the separator in a zinc-air battery is to transport the hydroxyl ion, OH^-, from the air electrode to the zinc electrode.[4] The basic requirements of a proper separator are stability in alkaline solution, appropriate pore size and porosity, high ionic conductivity and electrical non-conductivity. Since a zinc-air cell uses the migration of the hydroxyl ion, not the proton, H^+,[148] separators are made of polyethylene, polyvinyl alcohol, polyolefin, and polypropylene.[149–153] Porosity in the separator, however, makes it possible for the zinc cations to migrate from the anode to the cathode, which results in decreased capacity in the cell. Kiros developed a novel method to control the permeability of the zincate ion by introducing an inorganic material, $Mn(OH)_2$, to the microporous membrane.[154] Dewi et al. showed that cationic polysulfonium, poly(methylsulfonio-1,4-phenylenethio-1,4-phenylene trifluoromethanesulfonate) could be effectively applied to prevent the permeation of Zn^{2+} from the anode to the cathode, as shown in **Figure 10**, as compared to commercial separators such as polypropylene.[153] Wu et al. suggested that sulfonation of the microporous membrane could increase the high anionic transport number to 0.89 in a 1M KOH alkaline solution. This separator demonstrated better performance than the unsulfonated samples.[155] Besides the basic requirements mentioned above, others are needed for a viable secondary zinc-air battery; the separator should be inert to oxidation, and should remain stable during charge and discharge. Further, it needs high absorption for electrolytes and a fine porous structure to sustain electrolytes in the pores and retard zinc dendrite growth.[114]

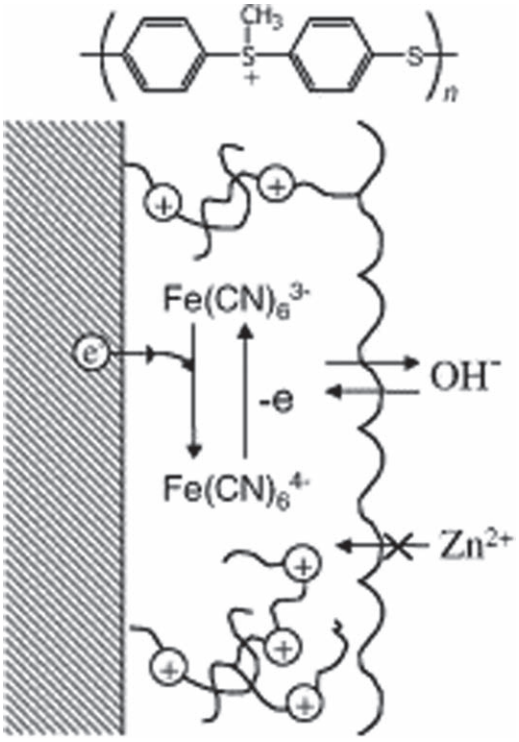

Figure 10. Scheme of modified electrode using polysufonium. Reprinted with permission.[153] Copyright 2003, Elsevier.

3.2.2. Electrolyte

The alkaline electrolytes used in zinc-air batteries are potassium hydroxide, sodium hydroxide, and lithium hydroxide,[2] all basic except for neutral NH_4Cl[156]. Among these, KOH has been widely used in zinc-air cells because of its superior ionic conductivity of K^+(73.50 Ω^{-1} cm^2/equiv) compared to Na^+(50.11 Ω^{-1} cm^2/equiv)[148] In addition, ~30% KOH is usually used because it shows maximum ionic conductivity at this concentration.[3] To reduce the resistance of the electrolyte, increasing the concentration of KOH can be a solution, but too high a concentration of KOH can lead to increased viscosity in the electrolyte. Besides this, high concentration of the electrolyte leads to the formation of ZnO, according to the reaction ($Zn(OH)_4^{2-} \rightarrow ZnO + H_2O + 2OH^-$), in turn increasing the viscosity.[148]

Because a zinc-air battery is operated in an alkaline solution and is exposed to air, the electrolyte is very sensitive to CO_2, which can react with hydroxyl ions to form carbonates;[157] concentration of the hydroxyl ion also decreases naturally during this process. Therefore, the carbonation of the alkaline electrolyte causes decreased cell capacity. Kim et al. reported that the concentration of potassium carbonate in the electrolyte caused a linear deterioration of cell capacity and that pore size of the hydrophobic membrane mainly affected the rate of carbon dioxide absorption.[158] Drillet et al. investigated the effect of CO_2 concentration in the air on the lifetime of the bifunctional electrode in alkaline solution by using solid adsorbents, including soda lime. In this study, an LiOH and LiOH-$Ca(OH)_2$ mixture was used to remove

CO_2. Further, they showed that increasing the concentration of carbon dioxide in synthetic air to 10000 ppm resulted in oxygen reducing electrodes rather than an oxygen evolving electrodes. They suggested that the reduced lifetime of the air electrode was due to carbonate precipitation inside the pores of the electrode.[159]

Chen et al. used the technique of combining chemical absorption with Higee (high gravity) as a CO_2-scrubber. They showed that under the same experimental conditions, piperazine (PZ) was more effective than 2-(2-aminoethylamino) ethanol (AEEA) and monoethanolamine (MEA) in reducing the concentration of CO_2 to a level below 20 ppm.[160]

3.3. Cathode: Air Electrode

The concept of using oxygen in a zinc-air battery requires the air electrode to have both proper catalysts for oxygen reduction reaction (ORR) and a highly porous structure. These two requirements should be considered simultaneously for designing an air electrode. As mentioned in the introduction, catalysts are needed to alleviate the large activation energy for ORR, but the structure of the air electrode is also an important factor affecting the performance of the zinc-air cell. In actual fact, the air electrode acts simply as a substrate where ORR occurs. Considering the overall reaction of the zinc-air battery ($2Zn + O_2 \rightarrow 2ZnO$), the only consumed materials are zinc metal and oxygen. Since oxygen is supplied endlessly from the atmosphere, in principle, the air electrode itself can be used repeatedly unless there is physical damage such as cracking in the air cathode after discharge.

3.3.1. Structure of Air Electrode

The highly porous structure of air electrodes makes a diffusion path for oxygen and functions as a substrate for catalysts. Therefore, carbon materials such as activated carbon and carbon nanotubes (CNT) can be used as substrates for the air electrode. Typically, an air electrode consists of a gas diffusion layer and a catalytic active layer and is prepared by laminating these together with a metal grid as a current collector.[161] (see Figure 7) The gas diffusion layer is composed of carbon material and a hydrophobic binder such as polytetrafluoroethylene (PTFE) as a wet-proofing agent. It is important to maintain hydrophobicity, which makes gas diffusion layer permeable to air but not water. The catalytic active layer consists of catalysts, carbon materials, and the binder. It is in the catalytic active layer that the oxygen reduction reaction (ORR) takes place. From the above discussion, it is reasonable to assume that types and amounts of each material[162] and structure of air electrode[163–166] affect the performance of the air electrode. Eom et al. reported that micropores (0.2 ~ 2 nm) of activated carbon did not affect the performance of the cathode in zinc-air batteries.[167] By placing carbon particles in a sinter-locked network of metal fibers, Zhu et al. developed a thin layer air electrode (<0.15 nm) that is 30 ~ 75% thinner than the commercial air electrode; they suggested that this structure makes the three-phase reaction sites more efficient.[112] To make a secondary zinc-air battery, developing a bifunctional catalyst is important. In addition to the catalyst itself, the oxidation of the catalyst [168] and the carbon substrate should also be considered in air electrodes where the oxygen evolution reaction (OER) takes place during charging, because the high surface area of the carbon substrate is severely attacked by the highly reactive oxygen generated from the OER.[157] Ross and Sattler demonstrated that graphitized carbon led to a reduction of the corrosion rate under anodic conditions in alkaline solutions.[169]

3.3.2. Catalysts

Although the oxygen reduction mechanism is very complex, it is believed that there are two kinds of mechanism. One is a direct four-electron pathway, in which oxygen directly reduces to OH^-; the other is a peroxide two-electron pathway, in which oxygen indirectly reduces to OH^- via HO_2^-.[134,170] Because the two-electron process is more common in alkaline solutions, proper catalysts are needed to facilitate the decomposition of HO_2^- into OH^-. It is well known that the kinetics of the oxygen reduction reaction (ORR) are very sluggish and that overpotential is required for the desired reaction. This phenomenon conversely decreases power density and high rate discharge. On the other hand, this problem is a commonly observed one in batteries using oxygen as active material, such as other metal-air cells and fuel cells. Therefore, many efforts to overcome this problem have focused on finding proper catalysts to reduce the oxygen reduction overpotential (see Figure 8).

Advances in computational catalysis have enabled us to screen inactive catalysts and to predict which catalysts will have more activity for ORR, which prediction helps save time and costs in developing proper catalysts. D-band center theory, suggested by Norskov, has played an important role in studies of catalysts,[171,172] and a famous volcano plot has been used to predict activity and selectivity of catalysts for ORR when designing better fuel cells[173] as shown in **Figure 11**. Based on this plot, many noble metal catalysts, both alloy and faced-metal catalysts, have been studied to improve

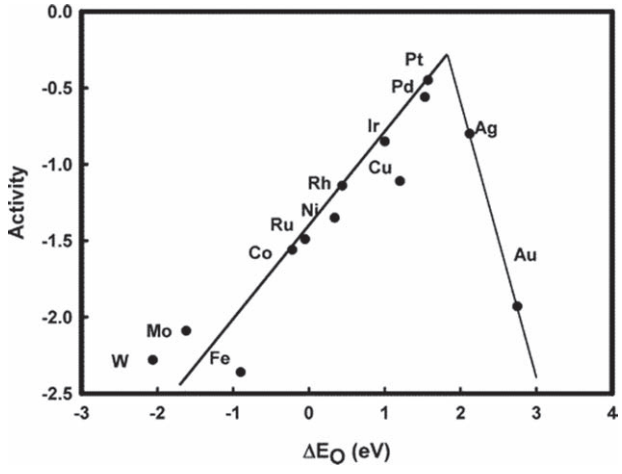

Figure 11. Trends in oxygen reduction activity (defined in the text) plotted as a function of the oxygen binding energy. Reprinted with permission.[173] Copyright 2004, American Chemical Society.

ORR activity.[174–181] Although noble metal catalysts such as platinum have high activity for ORR, the cost of manufacturing an air cathode increases dramatically when using such metals, which impedes commercialization. And, because oxygen reduction in alkaline solution is used as the cathode reaction in the zinc-air system, it is not necessary to use a pure noble metal catalyst.[157] With an advantage in the alkaline system, it is possible to use typical transition metal oxides such as perovskite, pyrochlore and spinel, individual oxides, and their mixtures for air cathodes.[157,170,182–184] Gorlin et al. reported that Mn oxide thin film showed higher activity for both ORR and OER, similar to that of noble metal catalysts: Pt, Ru, and Ir.[185] Han et al. reported on the dependence of particle size on the oxygen reduction reaction (ORR). Using cyclic voltammetry and a rotating disk electrode (RDE), they found that the direct four electron pathways were preferred by larger Ag particles (174 nm), and that simultaneous four electron and peroxide two-electron pathways were preferred by finer Ag particles (4.1 nm).[186] Recently, graphene has been used as an ORR catalyst without metal. Qu et al. showed that nitrogen-doped graphene (N-graphene) has much better activity than platinum for ORR via the four electron pathway in alkaline solution; it also has long-term operation stability.[187] **Figure 12** shows the preliminary rotating disk electrode (RDE) results at 3200 rpm for several samples including graphene oxide (GO) and MnOx composite. Although the limiting current of this sample is lower than that of commercial 20% Pt on carbon (E-tek), the current of the GO-MnOx composite is higher than those of commercial MnO_2. Since the composite thickness decreases to a very thin layer, we expect that battery performance may improve significantly upon optimization.

3.4. Design of Zinc-air Batteries

There are three main types of zinc air batteries: primary, secondary, and mechanically rechargeable cells.[114] Primary zinc-air cells are designed for single use. Therefore, they cannot be recharged electrically or mechanically. In other words, such cells are controlled by only zinc and the electrolyte.[114] What has been developed to overcome these limitations is a mechanically rechargeable zinc-air battery. In principle, the lifetime of such a cell depends on the air cathode, not on the anode or the electrolyte, because the utilized zinc and electrolyte can be replaced.[188,189] Another case is a combination of both a mechanically and an electrically rechargeable approach, that is, a slurry cell.[190–192] Such a cell uses a zinc suspension in an alkaline electrolyte. Besides the abovementioned charging methods, Wen et al. suggested that the introduction of propanol oxidation as a counter electrode reaction enhanced the electrical energy utilization.[193]

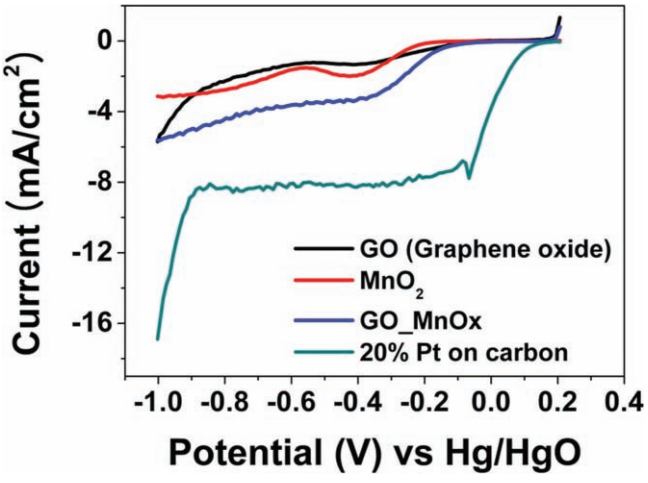

Figure 12. Rotating disk electrode experiments under 3200 rpm and 0.1 M KOH solution using GO (Graphene oxide), MnO_2, GO and MnOx composite, commercial 20% Pt on carbon (E-tek). Concentration of each sample is 2 mg/mL and scan rate is 10 mv/s.

For secondary zinc-air battery applications, in spite of some recent advances,[194,195] commercialization is still difficult because there are many problems, as mentioned in this article. To realize such cells, the first approach is to develop a reversible zinc anode with an understanding of the chemistry of the zincate ion in alkaline electrolytes. Secondly, proper and stable bifunctional catalysts for both ORR and OER are required. These catalysts can decrease the overpotential in the cathode, which will increase the Coulomb efficiency and also diminish the damage to the air electrode during charging. In addition, the air electrode should be further optimized to reduce resistance. Thirdly, proper carbon dioxide management and separators should also be developed. It is necessary to consider these obstacles simultaneously to develop commercial secondary zinc-air batteries in the future.

4. Conclusions

There has been promising progress in the area of Zn-air and Li-air batteries over the past decade. Promising electrochemical performance, low cost, and high energy density are factors that have driven research interest in these batteries. All components of Zn-air batteries are stable towards moisture, and thus the assembly of cells can be carried out under ambient air conditions. Therefore, it is much easier to handle Zn-air cells compared to Li-air batteries, because most components of Li-air cells are unstable towards moisture. Li-air cells must be assembled in an inert atmosphere. This implies that the manufacturing process of Zn-air batteries is simpler than that of Li-air batteries. Zn-air batteries also have stronger price competitiveness than Li-air batteries, because Zn metal and the aqueous electrolytes of Zn-air batteries are much cheaper than Li metal and the non-aqueous electrolytes of Li-air batteries. In addition, the technical level of Zn-air batteries is considered to be closer to practical application. However, the reversibility of Li-air batteries is better than that of Zn-air batteries, and the charging ability is a critical obstacle for the practical application of rechargeable Zn-air batteries. Also, the operating potential and specific capacity of Li-air batteries is higher than those of Zn-air batteries, resulting in much higher energy density, an irresistible fascination of Li-air batteries.

Although there has been promising progress, many aspects of Zn-air and Li-air batteries are not fully understood, and will require additional investigation. In this review, the fundamentals

and recent progress of work in the field of Li-air and Zn-air batteries have been highlighted. The following main points were addressed.

1. For Li-air batteries:

i) There are four types of Li-air batteries, based on the electrolyte used: 1) non-aqueous electrolyte, 2) aqueous electrolyte, 3) hybrid electrolyte, and 4) all-solid-state electrolyte.

ii) The electrode porosity affects the electrochemical performance of the air cathode. Oxygen diffusion is facilitated as the porosity increases, resulting in an improvement of the kinetics of the oxygen reduction reaction.

iii) Various catalysts have been investigated for the air cathode, and polarization has been substantially decreased by these catalysts. Each oxygen reduction reaction (ORR) and oxygen evolution reaction (OER) exhibits different catalytic reaction mechanisms, and thus a bifunctional catalyst is favorable to decrease the resistances of both reactions.

iv) The polarity, viscosity, and oxygen solubility of electrolytes are important factors affecting the electrochemical performance. Also, hydrophobic ionic liquids are promising electrolytes because they are immiscible in water.

v) Dendrite formation of Li metal causes poor cycle performance, but it can be suppressed by the formation of a stable SEI film on the surface of Li metal. The additives in electrolytes are effective at forming a stable SEI film.

2. For Zn-air batteries:

i) Zinc morphology can affect the electrochemical behavior of Zn-air batteries because zinc particles with high surface area can react efficiently with electrolytes. Also, the hydrogen evolution reaction (HER) is possible in a zinc anode operated in alkaline electrolyte, resulting in a decrease of the capacity of Zn-air batteries. To overcome this problem, coating, alloying, and adding additives to the electrolyte have been applied in this research area. To make a secondary battery, the most important point is to understand the chemistry of the zincate ion in alkaline solutions.

ii) The most critical problem in zinc-air batteries is still the sluggish reaction of oxygen chemistry originating from high overpotentials for both ORR and OER. Non-noble metal catalysts including perovskite, pyrochlore, and spinel play important roles in decreasing the overpotential in the air cathode. The architecture of air electrodes is also an important criterion affecting the overall performance of cathode electrodes.

iii) The migration of zinc(II) ions from anode to cathode can take place, which causes a decrease in the capacity of zinc-air batteries. Therefore, the pore size of the separator should be optimized to improve electrochemical performance. Carbonation in alkaline solution also has a negative effect on the lifetime of zinc-air cells. A CO_2 scrubber can be introduced to solve this problem.

Acknowledgements

This work was supported by the National Research Foundation of Korea (NRF) grant funded by the Korea government (MEST) (No. 2010–0019408 and WCU).

Received: October 25, 2010
Revised: November 15, 2010
Published online: December 8, 2010

[1] M. Armand, J. M. Tarascon, *Nature* **2008**, *451*, 652.
[2] P. Sapkota, H. Kim, *J. Ind. Eng. Chem.* **2009**, *15*, 445.
[3] F. R. McLarnon, E. J. Cairns, *J. Electrochem. Soc.*, *138*, 645.
[4] P. Arora, Z. J. Zhang, *Chem. Rev* **2004**, *104*, 4419.
[5] K. M. Abraham, Z. Jiang, *J. Electrochem. Soc.* **1996**, *143*, 1.
[6] T. Ogasawara, A. Debart, M. Holzapfel, P. Novak, P. G. Bruce, *J. Am. Chem. Soc.* **2006**, *128*, 1390.
[7] J. A. Zhang, W. Xu, X. H. Li, W. Liu, *J. Electrochem. Soc.* **2010**, *157*, A940.
[8] J. Kumar, B. Kumar, *J. Power Sources* **2009**, *194*, 1113.
[9] J. G. Zhang, D. Y. Wang, W. Xu, J. Xiao, R. E. Williford, *J. Power Sources* **2010**, *195*, 4332.
[10] Y. C. Lu, H. A. Gasteiger, M. C. Parent, V. Chiloyan, Y. Shao-Horn, *Electrochem. Solid State Lett.* **2010**, *13*, A69.
[11] C. O. Laoire, S. Mukerjee, K. M. Abraham, E. J. Plichta, M. A. Hendrickson, *J. Phys. Chem. C* **2009**, *113*, 20127.
[12] C. O. Laoire, S. Mukerjee, K. M. Abraham, E. J. Plichta, M. A. Hendrickson, *J. Phys. Chem. C* **2010**, *114*, 9178.
[13] J. S. Hummelshoj, J. Blomqvist, S. Datta, T. Vegge, J. Rossmeisl, K. S. Thygesen, A. C. Luntz, K. W. Jacobsen, J. K. Norskov, *J. Chem. Phys.* **2010**, *132*.
[14] F. Mizuno, S. Nakanishi, Y. Kotani, S. Yokoishi, H. Iba, *Electrochemistry* **2010**, *78*, 403.
[15] Y.-C. Lu, H. A. Gasteiger, E. Crumlin, J. R. McGuire, Y. Shao-Horn, *J. Electrochem. Soc.* **2010**, *157*, A1016.
[16] D. Aurbach, M. Daroux, P. Faguy, E. Yeager, *J. Electroanal. Chem.* **1991**, *297*, 225.
[17] M. J. Gibian, D. T. Sawyer, T. Ungermann, R. Tangpoonpholvivat, M. M. Morrison, *J. Am. Chem. Soc.* **1979**, *101*, 640.
[18] S. J. Visco, B. D. Katz, Y. S. Nimon, L. C. De Jonghe, *US Patent* 7282295 **2007**.
[19] S. J. Visco, Y. S. Nimon, *US Patent* 7645543 **2010**.
[20] Y. G. Wang, H. S. Zhou, *J. Power Sources* **2010**, *195*, 358.
[21] Y. G. Wang, H. S. Zhou, *Chem. Commun.* **2010**, *46*, 6305.
[22] T. Zhang, N. Imanishi, Y. Shimonishi, A. Hirano, J. Xie, Y. Takeda, O. Yamamoto, N. Sammes, *J. Electrochem. Soc.* **2010**, *157*, A214.
[23] S. Hasegawa, N. Imanishi, T. Zhang, J. Xie, A. Hirano, Y. Takeda, O. Yamamoto, *J. Power Sources* **2009**, *189*, 371.
[24] T. Zhang, N. Imanishi, S. Hasegawa, A. Hirano, J. Xie, Y. Takeda, O. Yamamoto, N. Sammes, *Electrochem. Solid State Lett.* **2009**, *12*, A132.
[25] T. Zhang, N. Imanishi, S. Hasegawa, A. Hirano, J. Xie, Y. Takeda, O. Yamamoto, N. Sammes, *J. Electrochem. Soc.* **2008**, *155*, A965.
[26] B. Kumar, J. Kumar, R. Leese, J. P. Fellner, S. J. Rodrigues, K. M. Abraham, *J. Electrochem. Soc.* **2010**, *157*, A50.
[27] M. Eswaran, N. Munichandraiah, L. G. Scanlon, *Electrochem. Solid State Lett.* **2010**, *13*, A121.
[28] D. Zhang, Z. H. Fu, Z. Wei, T. Huang, A. S. Yu, *J. Electrochem. Soc.* **2010**, *157*, A362.
[29] M. Mirzaeian, P. J. Hall, *J. Power Sources* **2010**, *195*, 6817.
[30] H. Cheng, K. Scott, *J. Power Sources* **2010**, *195*, 1370.
[31] J. Xiao, D. H. Wang, W. Xu, D. Y. Wang, R. E. Williford, J. Liu, J. G. Zhang, *J. Electrochem. Soc.* **2010**, *157*, A487.
[32] X. H. Yang, P. He, Y. Y. Xia, *Electrochem. Commun.* **2009**, *11*, 1127.

[33] J. P. Zheng, R. Y. Liang, M. Hendrickson, E. J. Plichta, *J. Electrochem. Soc.* **2008**, *155*, A432.
[34] G. Q. Zhang, J. P. Zheng, R. Liang, C. Zhang, B. Wang, M. Hendrickson, E. J. Plichta, *J. Electrochem. Soc.* **2010**, *157*, A953.
[35] S. D. Beattie, D. M. Manolescu, S. L. Blair, *J. Electrochem. Soc.* **2009**, *156*, A44.
[36] S. S. Sandhu, J. P. Fellner, G. W. Brutchen, *J. Power Sources* **2007**, *164*, 365.
[37] S. S. Sandhu, G. W. Brutchen, J. P. Fellner, *J. Power Sources* **2007**, *170*, 196.
[38] J. Read, K. Mutolo, M. Ervin, W. Behl, J. Wolfenstine, A. Driedger, D. Foster, *J. Electrochem. Soc.* **2003**, *150*, A1351.
[39] X. H. Yang, Y. Y. Xia, *J. Solid State Electrochem.* **2010**, *14*, 109.
[40] C. Tran, X. Q. Yang, D. Y. Qu, *J. Power Sources* **2010**, *195*, 2057.
[41] A. Debart, J. Bao, G. Armstrong, P. G. Bruce, *J. Power Sources* **2007**, *174*, 1177.
[42] A. Debart, A. J. Paterson, J. Bao, P. G. Bruce, *Angew. Chem. Int. Ed.* **2008**, *47*, 4521.
[43] Y. Xu, W. A. Shelton, *J. Chem. Phys.* **2010**, *133*.
[44] Y. C. Lu, Z. C. Xu, H. A. Gasteiger, S. Chen, K. Hamad-Schifferli, Y. Shao-Horn, *J. Amer. Chem. Soc.* **2010**, *132*, 12170.
[45] J. Read, *J. Electrochem. Soc.* **2002**, *149*, A1190.
[46] W. Xu, J. Xiao, J. Zhang, D. Y. Wang, J. G. Zhang, *J. Electrochem. Soc.* **2009**, *156*, A773.
[47] W. Xu, J. Xiao, D. Y. Wang, J. Zhang, J. G. Zhang, *J. Electrochem. Soc.* **2010**, *157*, A219.
[48] J. Xiao, W. Xu, D. Y. Wang, J. G. Zhang, *J. Electrochem. Soc.* **2010**, *157*, A294.
[49] P. Bonhote, A. P. Dias, N. Papageorgiou, K. Kalyanasundaram, M. Gratzel, *Inorg. Chem.* **1996**, *35*, 1168.
[50] T. Kuboki, T. Okuyama, T. Ohsaki, N. Takami, *J. Power Sources* **2005**, *146*, 766.
[51] D. Zhang, R. S. Li, T. Huang, A. S. Yu, *J. Power Sources* **2010**, *195*, 1202.
[52] M. Winter, J. O. Besenhard, M. E. Spahr, P. Novak, *Adv. Mater.* **1998**, *10*, 725.
[53] E. Peled, *J. Electrochem. Soc.* **1979**, *126*, 2047.
[54] E. Peled, D. Golodnitsky, G. Ardel, *J. Electrochem. Soc.* **1997**, *144*, L208.
[55] S. Shiraishi, K. Kanamura, Z. I. Takehara, *J. Appl. Electrochem.* **1999**, *29*, 869.
[56] S. P. S. Yen, D. Shen, R. P. Vasquez, F. J. Grunthaner, R. B. Somoano, *J. Electrochem. Soc.* **1981**, *128*, 1434.
[57] K. Nishikawa, Y. Fukunaka, T. Sakka, Y. H. Ogata, J. R. Selman, *J. Electroanal. Chem* **2005**, *584*, 63.
[58] S. S. Zhang, *J. Power Sources* **2006**, *162*, 1379.
[59] N. Munichandraiah, L. G. Scanlon, R. A. Marsh, *J. Power Sources* **1998**, *72*, 203.
[60] D. Aurbach, *J. Power Sources* **2000**, *89*, 206.
[61] D. Aurbach, Y. Talyosef, B. Markovsky, E. Markevich, E. Zinigrad, L. Asraf, J. S. Gnanaraj, H. J. Kim, *Electrochim. Acta* **2004**, *50*, 247.
[62] J. G. Thevenin, R. H. Muller, *J. Electrochem. Soc.* **1987**, *134*, 273.
[63] J. Yamaki, S. Tobishima, K. Hayashi, K. Saito, Y. Nemoto, M. Arakawa, *J. Power Sources* **1998**, *74*, 219.
[64] Y. S. Cohen, Y. Cohen, D. Aurbach, *J. Phys. Chem. B* **2000**, *104*, 12282.
[65] T. Tatsuma, M. Taguchi, M. Iwaku, T. Sotomura, N. Oyama, *Journal of Electroanalytical Chemistry* **1999**, *472*, 142.
[66] M. Mori, K. Naoi, *Electrochemistry* **1999**, *67*, 39.
[67] G. R. Zhuang, P. N. Ross, *J. Power Sources* **2000**, *89*, 143.
[68] D. P. Wilkinson, D. Wainwright, *J. Electroanal. Chem.* **1993**, *355*, 193.
[69] T. Hirai, I. Yoshimatsu, J. Yamaki, *J. Electrochem. Soc.* **1994**, *141*, 2300.
[70] T. Hirai, I. Yoshimatsu, J. Yamaki, *J. Electrochem. Soc.* **1994**, *141*, 611.
[71] V. R. Koch, *J. Electrochem. Soc.* **1979**, *126*, 181.
[72] M. Odziemkowski, D. E. Irish, *J. Electrochem. Soc.* **1992**, *139*, 3063.
[73] M. Odziemkowski, D. E. Irish, *J. Electrochem. Soc.* **1993**, *140*, 1546.
[74] D. Aurbach, A. Zaban, Y. Gofer, Y. E. Ely, I. Weissman, O. Chusid, O. Abramson, *J. Power Sources* **1995**, *54*, 76.
[75] K. M. Abraham, J. S. Foos, J. L. Goldman, *J. Electrochem. Soc.* **1984**, *131*, 2197.
[76] P. Novak, K. Muller, K. S. V. Santhanam, O. Haas, *Chem. Rev.* **1997**, *97*, 207.
[77] F. Croce, S. Panero, S. Passerini, B. Scrosati, *Electrochim. Acta* **1994**, *39*, 255.
[78] V. D. Pokhodenko, V. G. Koshechko, V. A. Krylov, *J. Power Sources* **1993**, *45*, 1.
[79] J. O. Besenhard, J. Gurtler, P. Komenda, *J. Power Sources* **1987**, *20*, 253.
[80] J. O. Besenhard, M. W. Wagner, M. Winter, A. D. Jannakoudakis, P. D. Jannakoudakis, E. Theodoridou, *J. Power Sources* **1993**, *44*, 413.
[81] D. Aurbach, A. Zaban, *J. Electrochem. Soc.* **1994**, *141*, 1808.
[82] D. Aurbach, O. Chusid, *J. Electrochem. Soc.* **1993**, *140*, L155.
[83] T. Osaka, T. Momma, T. Tajima, Y. Matsumoto, *J. Electrochem. Soc.* **1995**, *142*, 1057.
[84] E. Plichta, S. Slane, M. Uchiyama, M. Salomon, D. Chua, W. B. Ebner, H. W. Lin, *J. Electrochem. Soc.* **1989**, *136*, 1865.
[85] D. Aurbach, Y. Gofer, M. Benzion, P. Aped, *J. Electroanal. Chem.* **1992**, *339*, 451.
[86] T. Osaka, T. Momma, Y. Matsumoto, Y. Uchida, *J. Electrochem. Soc.* **1997**, *144*, 1709.
[87] S. Shiraishi, K. Kanamura, Z. Takehara, *J. Appl. Electrochem.* **1995**, *25*, 584.
[88] K. Kanamura, H. Tamura, S. Shiraishi, Z. Takehara, *J. Electroanal. Chem.* **1995**, *394*, 49.
[89] K. Kanamura, S. Shiraishi, Z. Takehara, *J. Electrochem. Soc.* **1996**, *143*, 2187.
[90] K. Kanamura, H. Takezawa, S. Shiraishi, Z. Takehara, *J. Electrochem. Soc.* **1997**, *144*, 1900.
[91] D. Aurbach, M. L. Daroux, P. W. Faguy, E. Yeager, *J. Electrochem. Soc.* **1987**, *134*, 1611.
[92] M. W. Wagner, C. Liebenow, J. O. Besenhard, *J. Power Sources* **1997**, *68*, 328.
[93] Y. Matsuda, M. Ishikawa, S. Yoshitake, M. Morita, *J. Power Sources* **1995**, *54*, 301.
[94] M. Mori, Y. Naruoka, K. Naoi, D. Fauteux, *J. Electrochem. Soc.* **1998**, *145*, 2340.
[95] D. P. Wilkinson, H. Blom, K. Brandt, D. Wainwright, *J. Power Sources* **1991**, *36*, 517.
[96] M. Ishikawa, Y. Takaki, M. Morita, Y. Matsuda, *J. Electrochem. Soc.* **1997**, *144*, L90.
[97] G. B. Appetecchi, F. Croce, L. Persi, F. Ronci, B. Scrosati, *Electrochimica Acta* **2000**, *45*, 1481.
[98] G. B. Appetecchi, S. Passerini, *Electrochimica Acta* **2000**, *45*, 2139.
[99] F. Croce, G. B. Appetecchi, L. Persi, B. Scrosati, *Nature* **1998**, *394*, 456.
[100] B. Kumar, L. G. Scanlon, *J. Power Sources* **1994**, *52*, 261.
[101] B. Kumar, J. D. Schaffer, M. Nookala, L. G. Scanlon, *J. Power Sources* **1994**, *47*, 63.
[102] S. Slane, M. Salomon, *Journal of Power Sources* **1995**, *55*, 7.
[103] Z. Takehara, Z. Ogumi, Y. Uchimoto, K. Yasuda, H. Yoshida, *J. Power Sources* **1993**, *44*, 377.

[104] N. S. Choi, Y. M. Lee, J. H. Park, J. K. Park, *J. Power Sources* **2003**, *119*, 610.
[105] Y. M. Lee, N. S. Choi, J. H. Park, J. K. Park, *J. Power Sources* **2003**, *119*, 964.
[106] N. S. Choi, Y. M. Lee, K. Y. Cho, D. H. Ko, J. K. Park, *Electrochem. Commun.* **2004**, *6*, 1238.
[107] N. S. Choi, Y. M. Lee, W. Seol, J. A. Lee, J. K. Park, *Solid State Ionics* **2004**, *172*, 19.
[108] T. Osaka, T. Momma, Y. Matsumoto, Y. Uchida, *J. Power Sources* **1997**, *68*, 497.
[109] Z. Takehara, *J. Power Sources* **1997**, *68*, 82.
[110] K. Kanamura, H. Tomura, S. Shiraishi, Z. I. Takehara, *J. Electrochem. Soc.* **1995**, *142*, 340.
[111] K. Kanamura, S. Shiraishi, Z. Takehara, *J. Electrochem. Soc.* **1994**, *141*, L108.
[112] W. H. Zhu, B. A. Poole, D. R. Cahela, B. J. Tatarchuk, *J. Appl. Electrochem.* **2003**, *33*, 29.
[113] T. P. Dirkse, D. J. Kroon, *J. Appl. Electrochem.* **1971**, *1*, 293.
[114] C. Chakkaravarthy, A. K. A. Waheed, H. V. K. Udupa, *J. Power Sources* **1981**, *6*, 203.
[115] L. F. Urry, *US Patent* 6,022,639 **1996**.
[116] N. C. Tang, *US Patent* 6,221,527 **1998**.
[117] J. Goldstein, *US Patent* 6,015,636 **2000**.
[118] C.-C. Yang, S.-J. Lin, *J. Power Sources* **2002**, *112*, 174.
[119] X. G. Zhang, *J. Power Sources* **2006**, *163*, 591.
[120] M. Minakshi, D. Appadoo, D. E. Martin, *Electrochemical and Solid-State Letters* **2010**, *13*, A77.
[121] G. Coates, N. A. Hampson, A. Marshall, D. F. Porter, *J. Appl. Electrochem.* **1974**, *4*, 75.
[122] T. G. COMPANY, *World Patent* WO01/890650 2002.
[123] T. Burchardt, *World Patent* WO2006/538111 6002.
[124] S. Müller, F. Holzer, O. Haas, *J. Appl. Electrochem.* **1998**, *28*, 895.
[125] R. Othman, W. J. Basirun, A. H. Yahaya, A. K. Arof, *J. Power Sources* **2001**, *103*, 34.
[126] K. Kim, Y.-H. Cho, S. W. Eom, H.-S. Kim, J. H. Yeum, *Mater. Res. Bull.* **2010**, *45*, 262.
[127] T. I. Devyatkina, Y. L. Gun'ko, M. G. Mikhalenko, *Russ. J. Appl. Chem.* **2001**, *74*, 1122.
[128] C. W. Lee, K. Sathiyanarayanan, S. W. Eom, M. S. Yun, *J. Power Sources* **2006**, *160*, 1436.
[129] C. Zhang, J. M. Wang, L. Zhang, J. Q. Zhang, C. N. Cao, *J. Appl. Electrochem.* **2001**, *31*, 1049.
[130] Y.-D. Cho, G. T.-K. Fey, *J. Power Sources* **2008**, *184*, 610.
[131] L. Zhu, H. Zhang, W. Li, H. Liu, *J. Phys. Chem. Solids* **2009**, *70*, 45.
[132] Y. Ein-Eli, M. Auinat, D. Starosvetsky, *J. Power Sources* **2003**, *114*, 330.
[133] C. W. Lee, K. Sathiyanarayanan, S. W. Eom, H. S. Kim, M. S. Yun, *J. Power Sources* **2006**, *159*, 1474.
[134] D. Linden, B. Thomas, Reddy, Handbook of batteries, 3rd edition, McGraw-Hill, **2001**.
[135] R. Renuka, S. Ramamurthy, L. Srinivasan, *J. Power Sources* **2000**, *89*, 70.
[136] I. Arise, Y. Fukunaka, F. R. McLarnon, *J. Electrochem. Soc.* **2006**, *153*, A69.
[137] T. P. Dirkse, *J. Electrochem. Soc.* **1981**, *128*, 1412.
[138] C. Cachet, B. Saidani, R. Wiart, *J. Electrochem. Soc.* **1992**, *139*, 644.
[139] Y.-H. Wen, J. Cheng, L. Zhang, X. Yan, Y.-S. Yang, *J. Power Sources* **2009**, *193*, 890.
[140] B. Sharifi, M. Mojtahedi, M. Goodarzi, J. Vahdati Khaki, *Hydrometallurgy* **2009**, *99*, 72.
[141] W.-J. Peng, Y.-Y. Wang, *J. Central South Univ. Technol.* **2007**, *14*, 37.
[142] M. V. Simicic, K. I. Popov, N. V. Krstajic, *J. Electroanal. Chem.* **2000**, *484*, 18.
[143] P. P. Trigueros, J. Claret, F. Mas, F. Sagués, *J. Electroanal. Chem.* **1991**, *312*, 219.
[144] R. E. F. Einerhand, W. H. M. Visscher, E. Barendrecht, *J. Appl. Electrochem.* **1988**, *18*, 799.
[145] J. Hendrikx, A. Van Der Putten, W. Visscher, E. Barendrecht, *Electrochimica Acta* **1984**, *29*, 81.
[146] K. I. Popov, M. G. Pavlović, M. D. Spasojević, V. M. Nakić, *J. Appl. Electrochem.* **1979**, *9*, 533.
[147] J. W. Diggle, R. J. Fredericks, A. C. Reimschuessel, *J. Materi. Sci.* **1973**, *8*, 79.
[148] P. Sapkota, H. Kim, *J. Ind. Eng. Chem.* **2010**, *16*, 39.
[149] L.-C. Hsu, D. W. Sheibley, *J. Electrochem. Soc.* **1982**, *129*, 251.
[150] D. W. Sheibley, M. A. Manzo, O. D. Gonzalez-Sanabria, *J. Electrochem. Soc.* **1983**, *130*, 255.
[151] A. Lewandowski, K. Skorupska, J. Malinska, *Solid State Ionics* **2000**, *133*, 265.
[152] C.-C. Yang, S.-J. Lin, *J. Power Sources* **2002**, *112*, 497.
[153] E. L. Dewi, K. Oyaizu, H. Nishide, E. Tsuchida, *J. Power Sources* **2003**, *115*, 149.
[154] Y. Kiros, *J. Power Sources* **1996**, *62*, 117.
[155] G. M. Wu, S. J. Lin, J. H. You, C. C. Yang, *Mater. Chem. Phys.* **2008**, *112*, 798.
[156] J. Jindra, J. Mrha, M. Musilová, *J. Appl. Electrochem.* **1973**, *3*, 297.
[157] L. Jörissen, *J. Power Sources* **2006**, *155*, 23.
[158] Nam-In Kim, Yong-Kook Choi, Woo-Tae Lee, *J. Korean Ind. Eng. Chem.* **1999**, *10*, 177.
[159] J. F. Drillet, F. Holzer, T. Kallis, S. Muller, V. M. Schmidt, *Phys. Chem. Chem. Phys.* **2001**, *3*, 368.
[160] H.-H. Cheng, C.-S. Tan, *J. Power Sources* **2006**, *162*, 1431.
[161] S. Müller, K. Striebel, O. Haas, *Electrochim. Acta* **1994**, *39*, 1661.
[162] Kim Jee Hoon, Seung Wook Eom, Moon Seong In, Yun Mun Soo, Kim Ju Yong, Yug Gyeong Chang, Park Jeong Hoo. *J. Korean Electrochem. Soc.* **2003**, *6*, 203.
[163] Z.-Q. Fang, M. Hu, W.-X. Liu, Y.-R. Chen, Z.-Y. Li, G.-Y. Liu, *Electrochim. Acta* **2006**, *51*, 5654.
[164] F. Xie, Z. Tian, H. Meng, P. K. Shen, *J. Power Sources* **2005**, *141*, 211.
[165] C.-C. Yang, *Int. J. Hydrogen Energy* **2004**, *29*, 135.
[166] N. Furuya, *J. Solid State Electrochem.* **2003**, *8*, 48.
[167] S.-W. Eom, C.-W. Lee, M.-S. Yun, Y.-K. Sun, *Electrochim. Acta* **2006**, *52*, 1592.
[168] C. Fierro, R. E. Carbonio, D. Scherson, E. B. Yeager, *Electrochim. Acta* **1988**, *33*, 941.
[169] P. N. Ross, M. Sattler, *J. Electrochem. Soc.* **1988**, *135*, 1464.
[170] V. Neburchilov, H. Wang, J. J. Martin, W. Qu, *J. Power Sources* **2010**, *195*, 1271.
[171] B. Hammer, J. K. Norskov, *Nature* **1995**, *376*, 238.
[172] E. Santos, W. Schmickler, *ChemPhysChem* **2006**, *7*, 2282.
[173] J. K. Nørskov, J. Rossmeisl, A. Logadottir, L. Lindqvist, J. R. Kitchin, T. Bligaard, H. Jónsson, *J. Phys. Chem. B* **2004**, *108*, 17886.
[174] J. Greeley, J. K. Nørskov, M. Mavrikakis, *Ann. Rev. Phys. Chem.* **2002**, *53*, 319.
[175] V. R. Stamenkovic, B. Fowler, B. S. Mun, G. Wang, P. N. Ross, C. A. Lucas, N. M. Markovic, *Science* **2007**, 1135941.
[176] K. Lee, M. Kim, H. Kim, *J. Mater. Chem.* **2010**, *20*, 3791.
[177] J. Greeley, I. E. L. Stephens, A. S. Bondarenko, T. P. Johansson, H. A. Hansen, T. F. Jaramillo, J. Rossmeisl, Chorkendorffl, J. K. Nørskov, *Nat. Chem.* **2009**, *1*, 552.
[178] J. Zhang, M. B. Vukmirovic, Y. Xu, M. Mavrikakis, R. R. Adzic, *Angew. Chem.* **2005**, *117*, 2170.
[179] T. H. Yu, Y. Sha, B. V. Merinov, W. A. Goddard, *J. Phys. Chem. C* **2010**, *114*, 11527.
[180] H. A. Gasteiger, S. S. Kocha, B. Sompalli, F. T. Wagner, *Appl. Catal. B: Environmental* **2005**, *56*, 9.

[181] Y. Ma, P. B. Balbuena, *Chem. Phys. Lett.* **2007**, *440*, 130.
[182] R. N. S. M. Hamdani, P. Chartier, *Int. J. Electrochem. Sci* **2010**, *5*, 556.
[183] V. Nikolova, P. Iliev, K. Petrov, T. Vitanov, E. Zhecheva, R. Stoyanova, I. Valov, D. Stoychev, *J. Power Sources* **2008**, *185*, 727.
[184] B. Wang, *J. Power Sources* **2005**, *152*, 1.
[185] Y. Gorlin, T. F. Jaramillo, *J. Am. Chem. Soc.* **2010**, *132*, 13612.
[186] J.-J. Han, N. Li, T.-Y. Zhang, *J. Power Sources* **2009**, *193*, 885.
[187] L. Qu, Y. Liu, J.-B. Baek, L. Dai, *ACS Nano* **2010**, *4*, 1321.
[188] J. Goldstein, I. Brown, B. Koretz, *J. Power Sources* **1999**, *80*, 171.
[189] M. Pinto, J. A. Colborn, *US Patent 6,706,433 B2* **2004**.
[190] A. J. Appleby, M. Jacquier, *J. Power Sources* **1976**, *1*, 17.
[191] K. F. Blurton, A. F. Sammells, *J. Power Sources* **1979**, *4*, 263.
[192] J. Goldstein, A. Meitay, *US Patent* 5206096 **1993**.
[193] Y.-H. Wen, J. Cheng, S.-Q. Ning, Y.-S. Yang, *J. Power Sources* **2009**, *188*, 301.
[194] RevoltTechnology, Zurich, Switzerland, http://www.revolttechnology.com (accessed Novemebr 2010).
[195] E. Deiss, F. Holzer, O. Haas, *Electrochimica Acta* **2002**, *47*, 3995.